Straight-ahead running of road vehicles - Analytical formulae including full tyre characteristics

Giampiero Mastinu[a], Alessandro Lattuada[a] and Giuseppe Matrascia[b]

[a]Politecnico di Milano, Department of Mechanical Engineering, via Privata Giuseppe La Masa 1, 20158 Milan, Italy
[b]Pirelli Tyre S.p.A., Viale Piero e Alberto Pirelli 25, 20126 Milan, Italy

ARTICLE HISTORY
Compiled October 1, 2018

ABSTRACT
During straight-ahead running, the longitudinal axis of road vehicles, notably cars, is not parallel to road axis. This occurrence is general and is due both to road cross slope (road banking) and to tyre characteristics, particularly ply-steer and conicity. In order to describe such a phenomenon, the paper develops a new and relatively simple analytical model. Despite the model is linear, the solution which is provided is exact, since straight-ahead motion occurs with small angles and both the elastokinematics of suspension system and tyre characteristics can be modelled by linearised equations.

The Handling Diagram theory is updated and completed by introducing the actual shifts of tyre characteristics influencing running at vanishing lateral acceleration.

The validation of the analytical expressions is performed by using a *MSC Adams*™ full model of a car. The lateral drift coming from the null steering manoeuvre is simulated by both the simple model and the full *MSC Adams*™ model, with satisfactory results. The same two models are used to simulate successfully the weave test.

A subjective-objective experimental test campaign provides preliminary substantiation of the ability of the derived formulae to describe tyre performance.

By means of the unreferenced analytical formulae developed in the paper, we allow, given the vehicle, the proper tyre design specification, and vice-versa. In particular, a formula is given to make null the steering torque during straight-ahead driving. The derived analytical formulae may provide a sound understanding of the straight-ahead running of road vehicles.

KEYWORDS
Vehicle pull; ply-steer; conicity; straight-motion; pull forces; steering pull; PRAT; residual aligning torque; vehicle drift; on-cent handling; road cross slope

1. Introduction

In general, on a normal road, when running straight-ahead, vehicles need to be slightly steered. "*Nuisance*" is the term that Pottinger juxtaposes to the vehicle pull issue [1]. Vehicle pull arises whenever the driver has to exert a discernible steering torque (called pull) in order for the vehicle to run straight-ahead. Nuisance occurs when the vehicle does not maintain the intended straight path, and a lateral deviation (called drift)

CONTACT G. Mastinu. Email: mastinu@mecc.polimi.it

occurs. Customers take for granted that the vehicle tracks straight and free of pull in absence of steering inputs and external disturbances. Vehicle pull, or nuisance, represents a key problem for automotive Original Equipment Manufacturers (OEMs), and it is often a crucial factor during approval tests with tyre manufacturers. The factors producing vehicle pull can be divided into:

- External factors, such as crosswind or road cross slope, that are part of the boundary conditions or environment in which the vehicle system operates.
- Internal factors, or vehicle system related parameters. Among them, a key role is played by tyre characteristics and chassis characteristics, namely suspension elastokinematics, wheel alignment and steering system settings. Additionally, vehicle unbalances (e.g. non-symmetric weight distribution, improper wheel alignment, dimensional tolerances) play a role.

In the paper we will focus on tyre characteristic and chassis nominal settings.

Obviously straight-ahead running can be simulated efficiently by multi-body models with many degrees of freedom. But, to understand the relevant parameters and the inter-relationships among them affecting straight-ahead running, analytical formulae are of crucial importance.

In the last decades, the relationships between tyre ply-steer, conicity and vehicle behaviour during straight ahead motion have been dealt with. Lindenmuth [2] indicated the existence of a relationship between vehicle pull and tyre conicity and ply-steer [1,3]. Topping [4] highlighted the origin of steady-state tyre-induced vehicle pull [1,5,6]. The subsistence of a considerable influence on ply-steer from tyre tread was pointed out experimentally by Matyja [7], and then corroborated with FEM studies performed by Mundl et al. [8] and Toyo Tire & Rubber Co., Ltd. [9,10]. In [3,11–13] the effect of suspension geometry on vehicle pull was studied, cross camber, cross caster and other suspension alignment tolerances were examined.

All of the cited papers do not resort to analytical modelling involving the description of elastokinematics and road cross slope effects. This, in our opinion, is crucial for establishing the actual influence of relevant parameters on performance. Furthermore, we address the tyre influence on the on-centre handling behaviour of the vehicle.Our contribution can focus on an analytical model because the straight-ahead running can be dealt with by means of a relatively simple linear model.

The paper is structured as follows. At first, we present the models that are used, a single-track model and a full vehicle model developed in *MSC Adams*™. Then we derive analytically the lateral slips at front and rear axles, respectively. Additionally, we validate the analytical model by comparing the results with the ones coming from the full *MSC Adams*™vehicle model. The paper ends dealing with how suspension parameters settings can influence straight-ahead running.

2. System models

2.1. Simple single-track model with unreferenced features

Figure 1 shows the single-track (or bicycle) vehicle model, employed to derive the equations of motion of a vehicle running straight-ahead or negotiating bends with very large radius.

The equations of motion of the single-track vehicle model are a simplified version of the ones reported in [14]: small lateral acceleration is expected, with negligible roll

angle. Constant longitudinal velocity u is assumed. The ordinary differential equations of motion read

$$\begin{cases} \nwarrow v: & \dot{v} = \frac{1}{m}(F_{y1} + F_{y2} + mg\varphi_r) - u\ r \\ \curvearrowright r: & \dot{r} = \frac{1}{I_z}(a_1 F_{y1} + M_{z1} - a_2 F_{y2} + M_{z2}) \end{cases} \tag{1}$$

The meaning of the symbols is clarified by inspection of Figure 1a.

The subscript i is used to distinguish between the front axle ($i = 1$) and the rear axle ($i = 2$). The sign convention adopted in this work is illustrated in Appendix C.

2.1.1. Analytical steady-state

Tyre characteristics, elastokinematics in the suspension and steering systems, load transfer and body roll are usually not considered in single-track models like the one depicted in Figures 1a-1b. However, these effects can be included in the single-track model with unreferenced features by adopting the effective axle cornering stiffness $C^*_{eff,i}$ [14,15]. The linear formulation of the equations of motion reported in [14,15] is extended in this paper in order to take into account '*pull forces*' [1], i.e. tyre ply-steer and conicity. Moreover, different characteristics are considered for left and right tyres. Such two different characteristics may be ascribed to current manufacturing tolerances or they can be induced by road cross slope φ_r (see Figure 2). For small lateral-slip angles α_i, the linear effective *i-axle* side force $F_{y,i}$ can be expressed as:

$$F_{y,i} = C^*_{eff,i} \cdot \alpha_i + F_{y0,i} \tag{2}$$

where $F_{y0,i}$ is due to ply-steer and conicity of the tyres, plus other effects as described hereafter.

$C^*_{eff,i}$ is the effective axle cornering stiffness, which can be expressed as [14,15]:

$$C^*_{eff,i} = \frac{2C_{F\alpha,i0}}{1 + C_{roll,i} - C_{susp,i} + C_{steer,i} + C^*_{\Delta F_z,i}} \tag{3}$$

with $C_{F\alpha,i0}$ defined as the mean value between left and right tyres' cornering stiffness:

$$C_{F\alpha,i0} = \frac{C_{F\alpha,i0L} + C_{F\alpha,i0R}}{2} \tag{4}$$

The derivation of Equation 3 is illustrated in Appendix A.

The superscript * is used to highlight the terms which are modified with respect to the ones appearing in [14,15]. The unreferenced features of the analytical model refer to tyres' ply-steer and conicity. The terms of Equation 3 are defined below

$$C_{roll,i} = \frac{2l}{l - a_i} \cdot \frac{h'}{k_{\varphi 1} + k_{\varphi 2} - mgh'}(\varepsilon_i C_{F\alpha,i0} + \tau_i C_{F\gamma,i0}) \tag{5a}$$

$$C_{susp,i} = 2C_{F\alpha,i0} \cdot c_{sf,i} \tag{5b}$$

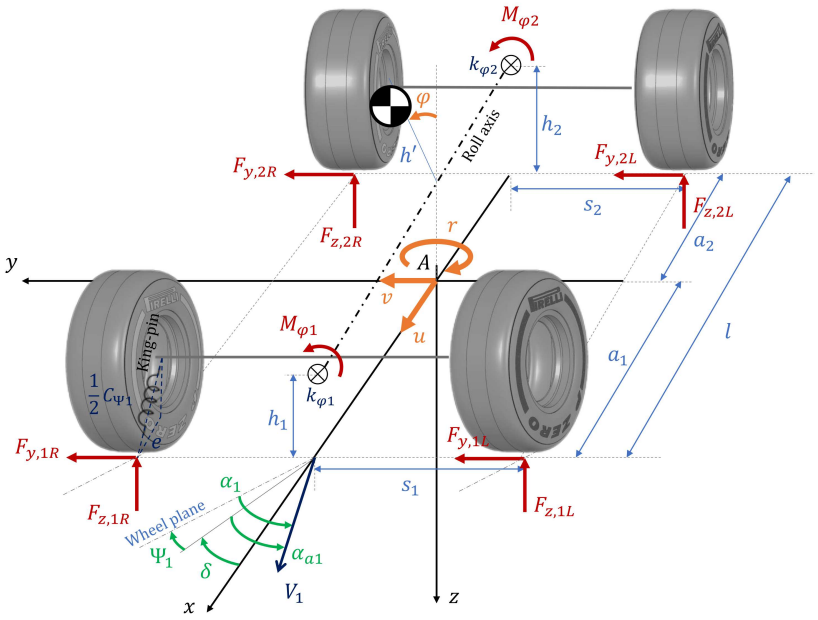

(a) Vehicle model showing the steering angle and axle's lateral-slip angle proper of the single-track model (adapted from [14]).

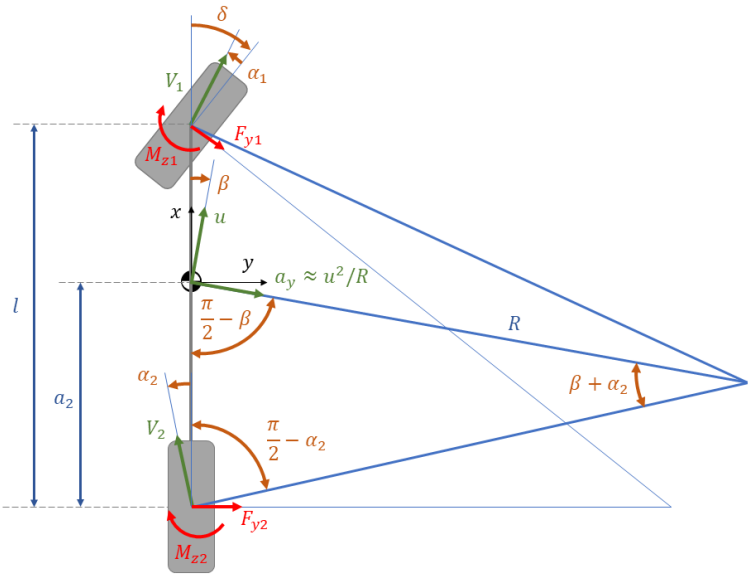

(b) Single-track vehicle model and vehicle side-slip β during circular driving (scheme adapted from [15]).

Figure 1. Simple vehicle model schemes.

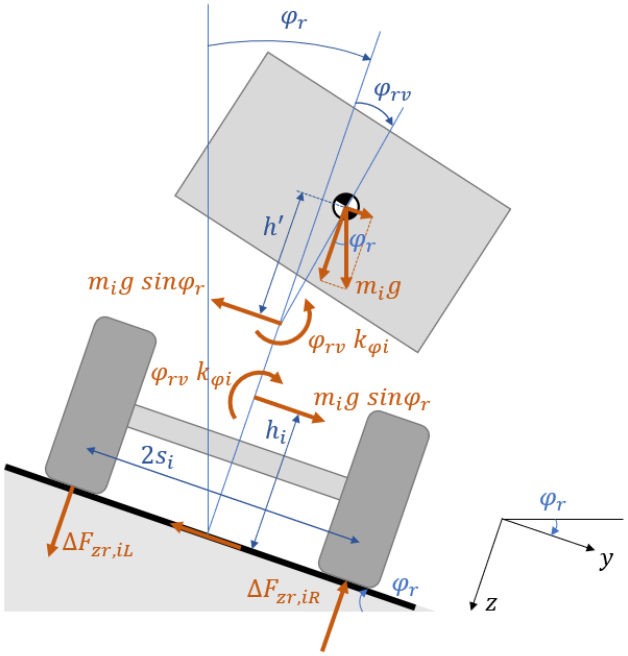

Figure 2. Vehicle scheme on a road with cross slope φ_r.

$$C_{steer,i} = 2C_{F\alpha,i0} \cdot \frac{n_i - t_{0,i}}{c_{\Psi,i}} \tag{5c}$$

$$\begin{aligned} C^*_{\Delta F_z,i} = \sigma_i \frac{l}{l-a_i} [&\xi_{\alpha,i}\,(2\Psi_{i0} - \alpha_{ply,iL} + \alpha_{ply,iR}) + \\ &+ \xi_{\gamma,i}\,(2\gamma_{i0} - \gamma_{con,iL} + \gamma_{con,iR})] \\ \text{where} \quad \sigma_i = \frac{1}{2s_i} &\left(\frac{k_{\varphi i}}{k_{\varphi 1} + k_{\varphi 2} - mgh'} h' + \frac{l-a_i}{l} h_i \right) \end{aligned} \tag{5d}$$

The values of the parameters appearing in Equation 5 are reported in Appendix D, and they are defined as follows:

l wheelbase
a_i distance between the CoG position and the i-axle
h' distance between roll axis and CoG
$k_{\varphi i}$ front/rear axis rolling stiffness
$\varepsilon_i = \frac{\Psi_{r,i}}{\varphi}$ front/rear roll-steering coefficient
$\tau_i = \frac{\gamma_{r,i}}{\varphi}$ front/rear roll-camber coefficient
$C_{F\alpha,i0}$ tyre's cornering stiffness
$C_{F\gamma,i0}$ tyre's side force camber coefficient
$c_{sf,i} = \frac{\Psi_{sf,i}}{F_{y,i}}$ suspension compliance
n caster offset
$t_0 = -\frac{C_{M\alpha}}{C_{F\alpha}}$ pneumatic trail
$c_{\Psi,i}$ steering stiffness around the king-pins
$\xi_{\alpha,i}$ coefficient of linearisation of $C_{F\alpha}(F_z)$ (see Appendix A)

$\xi_{\gamma,i}$ coefficient of linearisation of $C_{F\gamma}(F_z)$ (see Appendix A)
Ψ_{i0} toe angle
γ_{i0} camber angle

In Equation 5d, ply-steer equivalent lateral-slip angle α_{ply} and conicity equivalent camber angle γ_{con} are used, which are expressed according to [14] as:

$$\begin{aligned} \gamma_{con} &= \frac{\alpha_{FM0}}{\frac{C_{M\gamma}}{C_{M\alpha}} + \frac{C_{F\gamma}}{C_{F\alpha}}} \\ \alpha_{ply} &= \Delta\alpha_0 - \Delta\alpha_\gamma = \Delta\alpha_0 - \frac{C_{F\gamma}}{C_{F\alpha}}\gamma_{con} \end{aligned} \tag{6}$$

The parameters in Equation 6 can be written as function of the *Magic Formula* shifts [14]:

$$\begin{aligned} &\alpha_{FM0} = \frac{F_{y0}}{C_{F\alpha}} + \frac{M_{z0}}{C_{M\alpha}} = \frac{M_{zr0}}{C_{M\alpha}} \\ &\Delta\alpha_0 = \frac{F_{y0}}{C_{F\alpha}} = S_{Hf}|_{(\varphi=0,\gamma=0)} \\ &\text{where} \\ &C_{M\alpha} = K_{z\alpha 0} = D_{t0}K_{y\alpha}|_{\gamma=0} \\ &M_{zr0} = D_{r0} = F_z R_0(q_{Dz6} + q_{Dz7}\ df_z)\cdot\lambda_{Mr} \end{aligned}$$

The lateral force vertical shift $F_{y0,i}$ of Equation 2 includes both the contributions of tyre side force shifts $F_{y0,iL/R}$ and of proper (symmetric) wheel alignment (namely static toe Ψ_{i0} and static camber γ_{i0}), caused by the difference between left and right tyres' characteristics:

$$\begin{aligned} F_{y0,i} = C^*_{eff,i}\cdot\Bigg[&\Psi_{i0}\cdot\left(\frac{C_{F\alpha,i0R} - C_{F\alpha,i0L}}{C_{F\alpha,i0R} + C_{F\alpha,i0L}}\right) + \\ &+ \gamma_{i0}\cdot\left(\frac{C_{F\gamma,i0R} - C_{F\gamma,i0L}}{C_{F\alpha,i0R} + C_{F\alpha,i0L}}\right) + \left(\frac{F_{y0,iR} + F_{y0,iL}}{C_{F\alpha,i0R} + C_{F\alpha,i0L}}\right)\Bigg] \end{aligned} \tag{7}$$

The linear aligning moment characteristics, on the other hand, can be defined starting from left and right tyres' aligning moment stiffness $C_{M\alpha,iL/R}$ and offset $M_{z0,iL/R}$:

$$\begin{aligned} &M_{z,i} = -C_{M\alpha,i}\cdot\alpha_i + M_{z0,i} \\ &\text{where:} \\ &-C_{M\alpha,i} = -\left(C_{M\alpha,iL} + C_{M\alpha,iR}\right) \\ &M_{z0,i} = M_{z0,iL} + M_{z0,iR} \end{aligned} \tag{8}$$

The effects of road *cross slope* (or *road camber*) φ_r on vehicle system dynamics are introduced considering the induced body roll angle φ_{rv} and the related load transfer $\Delta F_{zr,i}$ (refer to Figure 2, with small angles approximation):

$$\varphi_{rv} = \frac{h'mg\cdot\varphi_r}{k_{\varphi 1} + k_{\varphi 2} - h'mg} \tag{9}$$

$$\Delta F_{zr,i} = \frac{1}{2s_i}\left[\frac{h' k_{\varphi i}}{k_{\varphi 1} + k_{\varphi 2} - h' mg} + \frac{l - a_i}{l} h_i\right] \cdot mg\varphi_r \tag{10}$$

The i-axle left and right wheel's static load (normal to the road surface) are

$$\begin{aligned} F_{z,iL,stat} &= \frac{1}{2}\left(mg \cdot \frac{l - a_i}{l}\right) - \Delta F_{zr,i} \\ F_{z,iR,stat} &= \frac{1}{2}\left(mg \cdot \frac{l - a_i}{l}\right) + \Delta F_{zr,i} \end{aligned} \tag{11}$$

The load transfer induced by road cross slope has an influence on cornering stiffness $C_{F\alpha,i0L/R}$, aligning moment stiffness $C_{M\alpha,iL/R}$, side force vertical shift $F_{y0,iL/R}$ and aligning moment shift $M_{z0,iL/R}$.

Furthermore, the road cross slope φ_r produces an additional lateral force $mg \cdot \varphi_r$, applied at the centre of mass and directed as the *y-axis* (refer to Figure 2). This force affects the handling diagram theory [14,15] in its linear range (valid for low lateral accelerations a_y).

Let us now re-formulate the Handling Diagram theory [14,15] by introducing the actual tyre characteristics, in which ply-steer and conicity are taken into account, together with road cross slope. Referring to Figure 1b, the new Handling Diagram equations read

$$\begin{cases} \frac{F_{y1} + (M_{z1} + M_{z2})/l}{F_{z1}} + \varphi_r = \frac{a_y}{g} \\ \\ \frac{F_{y2} - (M_{z1} + M_{z2})/l}{F_{z2}} + \varphi_r = \frac{a_y}{g} \end{cases} \tag{12}$$

where the axles' lateral forces F_{yi} and aligning moment M_{zi} can be expressed according to Equations 2 and 8, while the normal force on the i-axle is:

$$F_{zi} = mg \cdot \frac{l - a_i}{l} \tag{13}$$

2.1.2. Numerical model

The ordinary differential equations of motion of the single-track model (reported in Equation 1) are implemented in *MATLAB*® in order to simulate numerically the trajectory of the vehicle, substituting axles' side forces and aligning moments with Equations 2 and 8.

The axles' lateral-slip angles α_1 and α_2 are computed as [14]:

$$\begin{aligned} \alpha_1 &= \delta - \frac{v + a_1 r}{u} \\ \alpha_2 &= -\frac{v - a_2 r}{u} \end{aligned} \tag{14}$$

where δ is the steering angle at the wheels, which is linked to the steering wheel angle δ_{sw} by the average steering ratio n_{st}:

$$\delta = \frac{\delta_{sw}}{n_{st}} \tag{15}$$

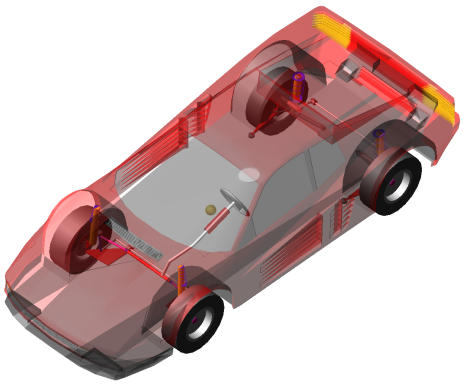

Figure 3. Full vehicle model in *MSC Adams*™.

2.2. Full vehicle model

A full vehicle model is developed with the multibody dynamics simulation software *MSC Adams*™. It has 49 Degrees of Freedom (DOFs) and it is represented in Figure 3. The objective is the validation of the analytical expressions and of the numerical results obtained with the single-track vehicle model.

The software *MSC Adams*™ automatically derives the non-reduced Newton-Euler equations of motion for the multibody system, in the form reported by [16]. The resulting Differential Algebraic Equations (DAEs) are solved numerically within *MSC Adams*™ by means of dedicated integration codes [16].

A *Roll & Vertical Force Analysis* of front McPherson and rear Multi-link suspension systems has been employed to estimate the elastokinematic coefficients of Equation 5. Their values are reported in Appendix D.

3. Analytical formulae

Equations 2 and 8 (and their related equations) can be substituted into Equation 12 in order to obtain a system of two equations and two unknowns, which are the lateral-slip angles α_1 and α_2:

$$\begin{cases} \mathrm{f}(\alpha_1, \alpha_2) = \frac{a_y}{g} - \varphi_r \mathrm{g}(\alpha_1, \alpha_2) = \frac{a_y}{g} - \varphi_r \end{cases} \tag{16}$$

The solution of the system is given by the front and rear axles' lateral-slip angles:

- Front lateral-slip angle (α_2):

$$\alpha_1 = K_{\alpha 1} \cdot \left(\frac{a_y}{g} - \varphi_r \right) + \alpha_{1,st}$$

$$K_{\alpha 1} = \frac{lF_{z1}C^*_{eff,2} + C_{M\alpha,2}mg}{lC^*_{eff,1}C^*_{eff,2} - C_{M\alpha,1}C^*_{eff,2} + C_{M\alpha,2}C^*_{eff,1}} \approx \frac{F_{z1}}{C^*_{eff,1}}$$

$$\alpha_{1,st} = \frac{-C^*_{eff,2}(M_{z0,1} + M_{z0,2} + lF_{y0,1}) - C_{M\alpha,2}(F_{y0,1} + F_{y0,2})}{lC^*_{eff,1}C^*_{eff,2} - C_{M\alpha,1}C^*_{eff,2} + C_{M\alpha,2}C^*_{eff,1}} \approx -\frac{F_{y0,1}}{C^*_{eff,1}} \tag{17}$$

- Rear lateral-slip angle (α_2):

$$\alpha_2 = K_{\alpha 2} \cdot \left(\frac{a_y}{g} - \varphi_r \right) + \alpha_{2,st}$$

$$K_{\alpha 2} = \frac{lF_{z2}C^*_{eff,1} - C_{M\alpha,1}mg}{lC^*_{eff,1}C^*_{eff,2} - C_{M\alpha,1}C^*_{eff,2} + C_{M\alpha,2}C^*_{eff,1}} \approx \frac{F_{z2}}{C^*_{eff,2}} \tag{18}$$

$$\alpha_{2,st} = \frac{C^*_{eff,1}(M_{z0,1} + M_{z0,2} - lF_{y0,2}) + C_{M\alpha,1}(F_{y0,1} + F_{y0,2})}{lC^*_{eff,1}C^*_{eff,2} - C_{M\alpha,1}C^*_{eff,2} + C_{M\alpha,2}C^*_{eff,1}} \approx -\frac{F_{y0,2}}{C^*_{eff,2}}$$

The approximations in Equations 17-18 have been introduced due to the considerably smaller value of the terms related to stiffness and offset of aligning moment with respect to the ones referred to side force.

The formulae of α_1 and α_2 (expressed by Equations 17-18) are derived for small lateral acceleration values (in this paper $a_y < 0.3g$ with $\mu \approx 1$) . In this range, the computed lateral-slip angles can be considered actual, non-approximated values, since the kinematic and elastokinematic effects have been included in their respective linearised expressions.

Once obtained the axles' lateral-slip angles α_1 and α_2, it is possible to derive easily the steering angle δ, the vehicle side-slip angle β and the steering torque M_S.

3.1. Steering angle

During circular driving at constant speed, the *Ackermann-angle* $\delta_0 = \frac{l}{R}$ can be expressed as function of lateral acceleration a_y. By introducing the centripetal acceleration $a_y = \frac{u^2}{R}$:

$$\delta_0 = \frac{l}{R} = \left(\frac{l \cdot g}{u^2} \right) \cdot \frac{a_y}{g} = \left(\frac{l \cdot g}{u^2} \right) \cdot \frac{a_y}{g}$$

Hence, the steering angle δ can be computed as:

$$\begin{aligned}\delta = \delta_0 + \alpha_1 - \alpha_2 = K_\delta \cdot \frac{a_y}{g} + \delta_{st} = \\ = (K_{\alpha 1} - K_{\alpha 2}) \cdot \left(\frac{a_y}{g} - \varphi_r\right) + \frac{l \cdot g}{u^2} \cdot \frac{a_y}{g} + (\alpha_{1,st} - \alpha_{2,st})\end{aligned} \tag{19}$$

The expressions pertaining to the straight motion of the vehicle are obtained from Equations 17-19 by imposing $a_y = 0$. In particular, the straight-driving steering angle offset can be defined from Equation 19 as $\delta_{st} = \delta(a_y = 0)$.

3.2. Vehicle side-slip angle

The vehicle side-slip angle β can be computed, under the assumption of small angles, as

$$\beta = -\alpha_2 + \frac{a_2}{R} \tag{20}$$

In the straight-ahead motion condition (thus with curve radius $R \to \infty$), vehicle side-slip angle becomes:

$$\beta_{st} = -\alpha_{2,st} + K_{\alpha 2} \cdot \varphi_r \tag{21}$$

3.3. Steering torque

The torque M_S that the driver has to apply to steer or to hold the steering wheel is the main factor that influences the steering feedback, transmitted from tyres to the steering wheel via the steering system [17] (see Figure 4). Following the simplified approach described in [18], the steering wheel torque M_S can be computed as:

$$M_S = \frac{F_{y1} \cdot n - M_{z1}}{n_{st} \cdot V_S} = \frac{M_S^*}{n_{st} \cdot V_S} \tag{22}$$

In Equation 22, n_{st} is the total steering gear ratio, accounting both for steering gear and linkage, and V_S is the steering gain (or steering assistance ratio) of the power steering system. This gain is inversely dependent on vehicle's velocity. For a highway driving condition, V_S can be assumed unitary [19]. In the above Equation we do not consider the influence of vertical forces that appear to provide a minor contribution, especially at small lateral-slip angles, proper of straight-ahead driving. More refined models for M_S can be found in [20].

In the following, we will focus on M_S^* calling it *steering torque*. M_S^* is the torque at the wheels (or, better, at the steering linkage side), that generates the torque M_S perceived by the driver. Due to this assumption, in our theoretical derivation we will not have to focus on the actual -strongly non linear- behaviour of the steering system. So we can resort plainly and rigorously on linearisation.

It is possible to include Equations 2, 8 and 17-19 into Equation 22, to write the steering torque M_S^* (where the superscript * indicates here the torque on the steering

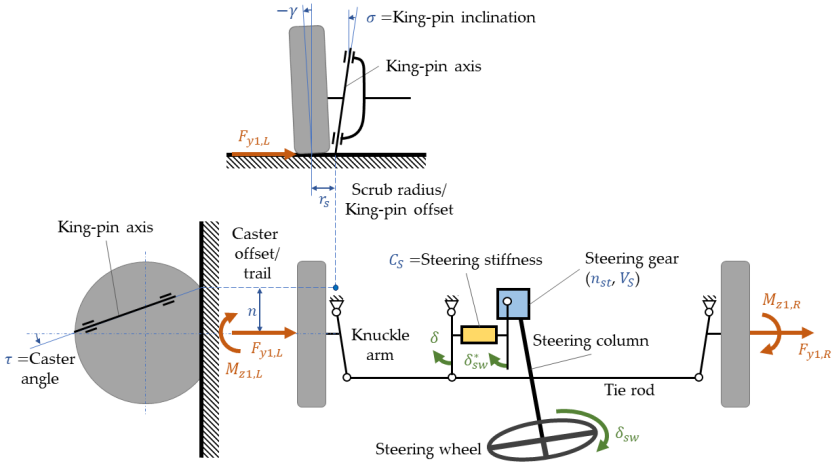

Figure 4. Scheme of steering system (adapted from [19,21,22]).

linkage side of the steering gear) as function of lateral acceleration a_y:

$$M_S^*(a_y) = \left(\frac{a_y}{g} - \varphi_r\right) \cdot K_{\alpha 1} \cdot \left[C^*_{eff,1} \cdot n + C_{M\alpha,1}\right] + n \cdot \left(C^*_{eff,1} \cdot \alpha_{1,st} + F_{y0,1}\right) + \\ + C_{M\alpha,1} \cdot \alpha_{1,st} - M_{z0,1R} - M_{z0,1L} \tag{23}$$

The straight-driving steering torque offset can be defined as $M^*_{S,st} = M^*_S(a_y = 0)$.

4. Validation

The validation of the derived analytical formulae is mainly theoretical. However, a preliminary subjective-objective evaluation is addressed which substantiates the ability of the formulae to describe tyre performance.

4.1. Validation of analytical formulae for describing straight-ahead driving

The full vehicle model in *MSC Adams*™ is employed to validate the analytical expressions for lateral-slip angles α_i, vehicle side-slip angle β and steering torque M_S for the straight-driving condition ($a_y = 0$).

The validation is carried out by means of simulations in *MSC Adams*™ of *Straight-Line event*, *Maintain* type, selecting the *steering input* option *straight line*. In this kind of simulation, the software determines the steering input that maintains the vehicle along a straight path. The simulations are performed on the full vehicle model equipped with the *Normal* set of tyres (see Appendix B), running at a constant velocity $u = 100\ km/h$, both with null and non-null road cross slope φ_r.

The analysis is conducted by comparing the analytical results with the final value assumed by five outputs of the *MSC Adams*™ simulations, after the initial transient part is completed and the vehicle is running straight:

- front lateral-slip angles: the lateral-slip angles of left and right front tyres, result-

ing from *MSC Adams*™ simulation, are compared with the front axle's straight-motion lateral-slip angle expressed by Equation 17:

$$\alpha_1 = -K_{\alpha 1} \cdot \varphi_r + \alpha_{1,st}$$

- rear lateral-slip angles: the lateral-slip angles of left and right rear tyres, resulting from *MSC Adams*™ simulation, are compared with the rear axle's straight-motion lateral-slip angle expressed by Equation 18:

$$\alpha_2 = -K_{\alpha 2} \cdot \varphi_r + \alpha_{2,st}$$

- lateral velocity: the lateral velocity assumed by the *MSC Adams*™ vehicle during straight-driving is analytically computed as the product between straight-motion vehicle side-slip angle and longitudinal velocity:

$$v_y = \beta_{st} \cdot u$$

- yaw angle: the yaw angle of the *MSC Adams*™ vehicle during straight-driving is compared with the rear axle's straight-motion lateral-slip angle expressed by Equation 18, which is opposite to the straight-motion vehicle side-slip angle expressed by Equation 21:

$$\Psi = -\beta_{st} = \alpha_2$$

- steering torque: the torque on the steering linkage side of the steering gear M_S^*, computed from *MSC Adams*™ simulation results is compared with the straight-motion analytical expression of $M_{S,st}^*$ of Equation 23.

$$M_S^* = (F_{y1,L} + F_{y1,R}) \cdot n - (M_{z1,L} + M_{z1,R})$$

The results of the simulation of the full vehicle model are reported in Figure 5, together with the results of the analytical expressions (dotted lines). As it can be observed, after the end of the transient part (caused by the initial conditions on *MSC Adams*™, which dictate null lateral-slip angles), the values from the full vehicle simulation have a considerable correspondence with the analytical results, both without and with road cross slope φ_r.

4.2. Validation of the numerical single-track model for describing lateral drift

In this section, the single-track vehicle model is validated by means of simulations performed with the *MSC Adams*™ full vehicle model, by comparing the resulting trajectories.

A *null steer test* is adopted, which can be defined as a particular kind of *fixed control test*, where the vehicle is maintained at a constant velocity of $u = 100\ km/h$ with steering wheel held fixed ($\delta_{sw} = \delta \cdot n_{st} = 0$). It is simulated with both the single-track model and the full vehicle model, with the different tyre sets available (see Appendix B). The deviation from the straight path (*drift* Δy) after 100 m from

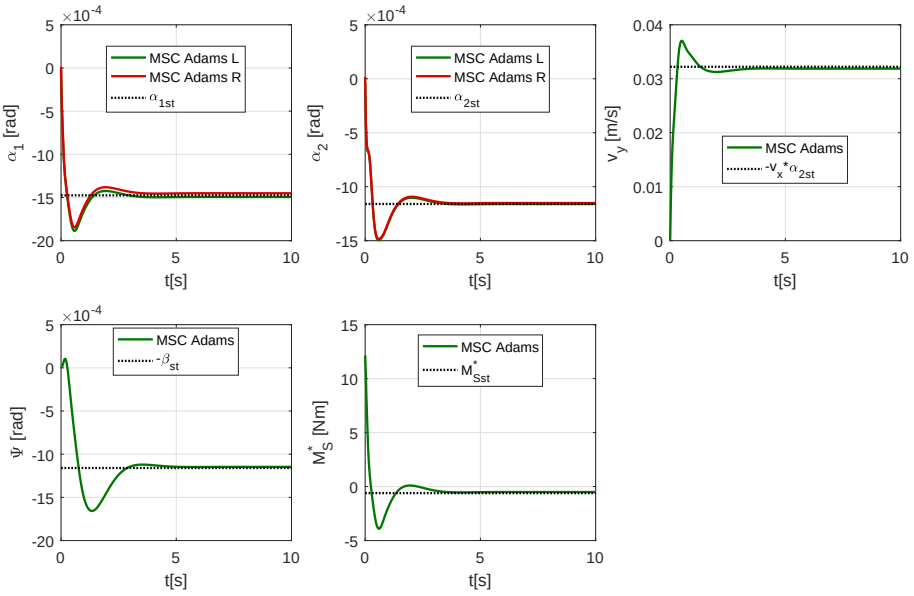

(a) Without road cross slope ($\varphi_r = 0$).

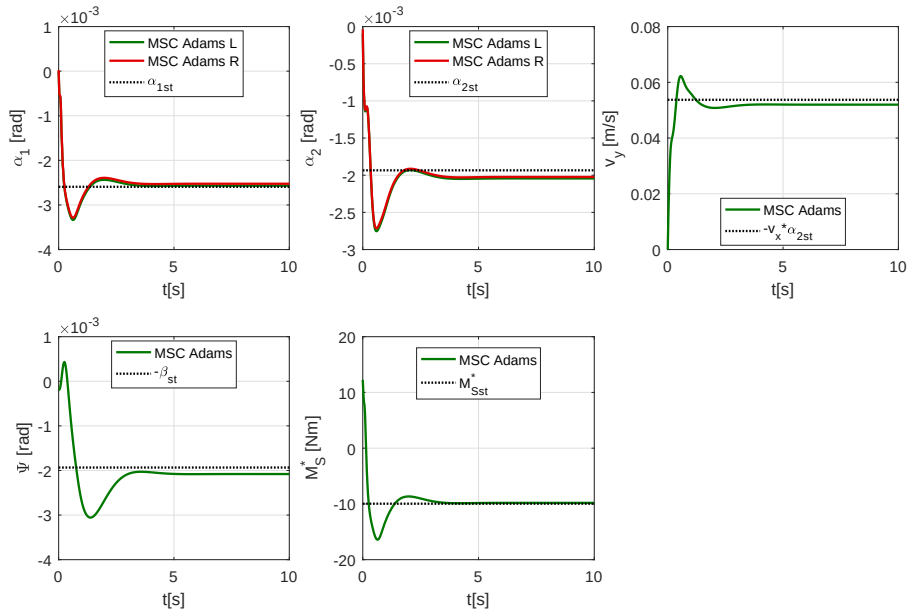

(b) With road cross slope ($\varphi_r = 0.02\ rad$).

Figure 5. Comparison between straight line maintaining test results in *MSC Adams*™ and analytical results (dotted lines). Vehicle equipped with *Normal* set of tyres (see data in Appendix B). Vehicle running at constant speed $u = 100\ km/h$.

Table 1. Results of the null steer test trajectories, simulated with single-track model with the four sets of tyres.

Tyre set	φ_r $[rad]$	Δy drift at $x = 100m$ $[m]$	δ_{st} $[10^{-4}\ rad]$	$M^*_{S,st}$ $[Nm]$
Normal	0.00	0.456	−3.151	−0.605
Mod-A	0.00	0.585	−4.259	−5.135
Mod-B	0.00	0.242	−1.379	3.606
Buffed	0.00	0.320	−2.129	3.138
Normal	0.02	0.923	−6.589	−9.958
Mod-A	0.02	1.042	−7.626	−14.695
Mod-B	0.02	0.699	−4.715	−6.069
Buffed	0.02	0.877	−6.838	−10.763

the point of steering wheel control (origin) is adopted as an index of vehicle unbalance, caused for instance by tyre pull forces.

The powertrain is detached in the full vehicle model, in order to conduct a free rolling analysis, isolating from the influence of longitudinal forces. Moreover, the motion resistances (namely tyre rolling resistance torque and aerodynamic drag) are nullified to maintain constant longitudinal velocity and avoid any load transfer which is not taken into account by the simple single-track model.

The *null steer test* is simulated both on a flat road and on a road with cross slope $\varphi_r = 0.02\ rad$. In the latter case, the road centreline in *MSC Adams*™is modelled so that it matches the trajectory of the vehicle. In this way, the road cross slope experienced by the vehicle is constant throughout the simulation, as imposed for the single-track model. Moreover, an additional term is introduced in the single-track model for the axles' side force $F_{y,i}$: the road cross slope-induced static vehicle roll $\varphi_{rv} = 0.0016\ rad$, which is computed as in Equation 9, causes a static inclination of the tyres:

$$\gamma_{roll,i} = \tau_i \cdot \varphi_{rv} \tag{24}$$

where $\tau_i = \gamma_{r,i}/\varphi$ is the roll-camber coefficient. Thus, each *i-axle* can account for an additional lateral force contribution, given by the normal load projection (since for small angles the tyres' lateral force camber coefficient may be assumed $C_{F\gamma} = F_z$):

$$F_{yi,tot} = F_{y,i} + \gamma_{roll,i} \cdot F_{z,i} \tag{25}$$

The results of the numerical simulations are shown in Figure 6 and reported in Table 1. As it can be observed, the trajectories obtained with the simple single-track model match the results simulated with the full vehicle model, both with and without road cross slope.

Furthermore, in a *null steer test* the smaller is the straight-driving steering angle δ_{st} (analytically computed according to Equation 19), the smaller is the drift, as it can be observed in Table 1. The straight-driving steering torque $M^*_{S,st}$ (Equation 23), on the other hand, does not have any influence on the trajectory in a *fixed* or *null steer test*: it affects the torque M_S that the driver has to apply on the steering wheel. It becomes relevant for the trajectory just in a *free control test*, when the steering wheel is released.

In addition, the results reported in Table 2 make it evident that suspension and steering system elastokinematics must be taken into account (*complete single-track*) in

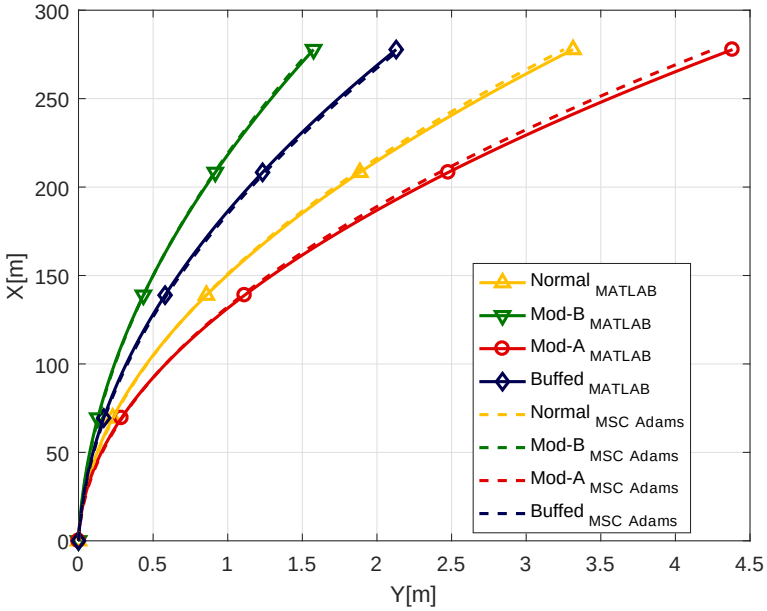

(a) Without road cross slope ($\varphi_r = 0$).

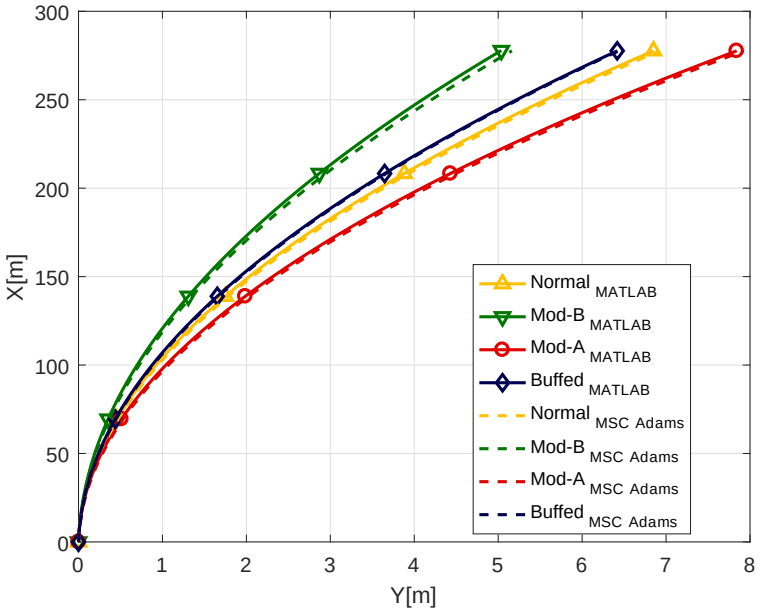

(b) With road cross slope ($\varphi_r = 0.02\ rad$).

Figure 6. Comparison between the trajectories simulated by single-track model and full vehicle model for a null steer test ($u = 100\ km/h$, $t = 10\ s$).

Table 2. Results of the null steer test trajectories, comparison between the single-track vehicle model with the elastokinematic effects (*complete*) and without the effective axle characteristics (*simplified*). Errors with respect to the *MSC Adams*™ full vehicle model results[a].

Tyre set	φ_r $[rad]$	Δy drift at $100m$						
		MSC Adams™	Complete single-track			Simplified single-track		
		Value $[m]$	Value $[m]$	Absolute error $[m]$	Relative error	Value $[m]$	Absolute error $[m]$	Relative error
Normal	0.00	0.459	0.456	0.003	0.7%	0.510	0.051	11.1%
Mod-A	0.00	0.583	0.585	0.002	0.3%	0.650	0.067	11.5%
Mod-B	0.00	0.244	0.242	0.002	0.8%	0.266	0.022	9.0%
Buffed	0.00	0.327	0.320	0.007	2.1%	0.356	0.029	8.9%
Normal	0.02	0.946	0.923	0.023	2.4%	0.837	0.109	11.5%
Mod-A	0.02	1.070	1.042	0.028	2.6%	0.967	0.103	9.6%
Mod-B	0.02	0.723	0.699	0.024	3.3%	0.581	0.142	19.6%
Buffed	0.02	0.888	0.877	0.011	1.2%	0.780	0.108	12.2%

order to have agreement between the full vehicle simulations and the single-track model results. Indeed, the elastokinematics modifies the effective axle side force, which is a key parameter for the trajectory. In case the elastokinematics effect is not considered (*simplified single-track*), the results of the single-track model still show correct trend with respect to the full vehicle simulations, but the description is not quantitatively accurate, as it can be inferred from the values of relative error reported in Table 2.

4.3. Subjective-objective experimental validation

In an experimental test campaign, the four tyres were considered. The data of the tyres are reported in Appendix B. The *Normal* set of tyres is the reference one. We have *Mod-A* and *Mod-B* tyres that have positive and negative PRAT respectively. For a comparison, we also have *Buffed* tyres. For sake of space we cannot report here the whole set of experimental tests in which a subjective-objective evaluation was performed.

The overall result was that *Mod-B* tyre was the very best, especially for steering feel at straight-ahead driving. *Mod-A* tyre was the worst one.

We can attempt an interpretation of such a result by inspecting Table 1. We see that, referring to the banked road ($\varphi_r = 0.02rad$), *Mod-B* tyre has the least values of drift, steering angle and steering torque with respect to other tyres. The opposite occurs for *Mod-A* tyre.

In our opinion this is a clue that could suggest the utility of the derived analytical formulae.

5. On-centre handling

A *weave test* [23,24] is simulated with the full vehicle model in order to analyse the on-centre handling. In this way, the influence of tyre characteristics on the on-centre vehicle behaviour is studied using objective metrics from the output results.

An adjusted *weave test*, similar to the one adopted in the study of Salaani et al. [23], is performed through an *open-loop sine steer event* in *MSC Adams*™ with:

- low speed: $u = 50\ km/h$
- small steering wheel displacement amplitude: $|\delta_{sw}| = 20\,\text{deg}$

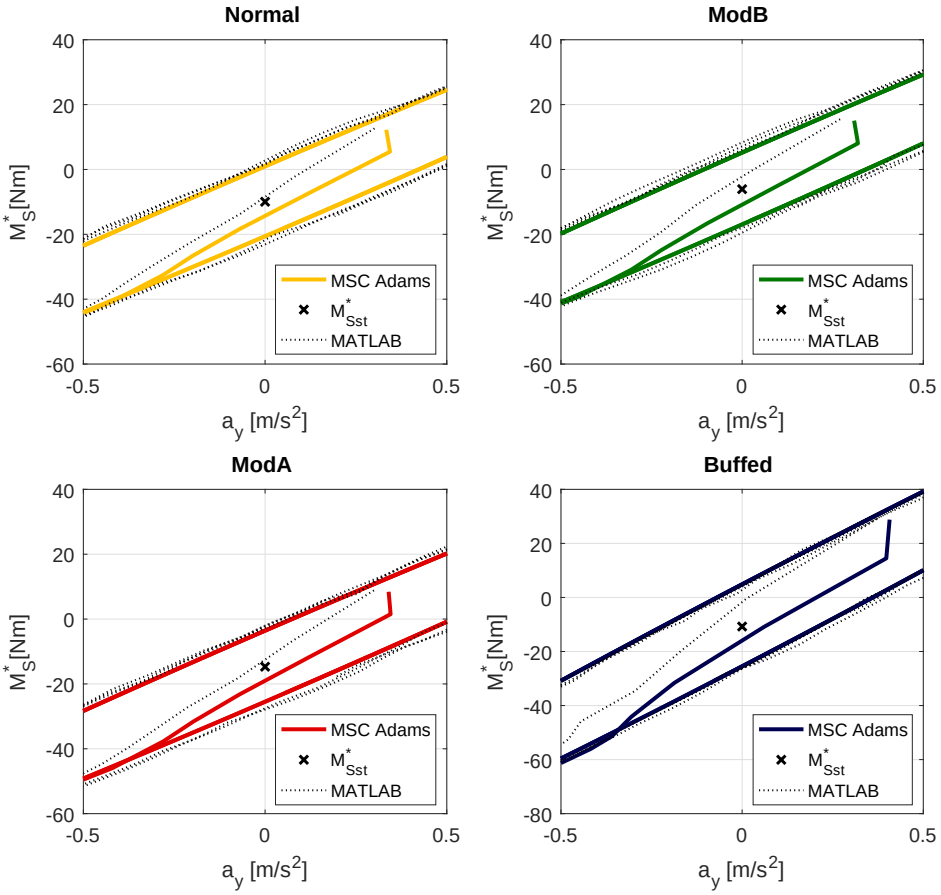

Figure 7. Weave test simulation with different tyres (see Appendix B). Steering torque vs lateral acceleration. Road cross slope $\varphi_r = 0.02$ *rad*. The cross represents the analytically computed steering torque offset, and shows correspondence with the centre of the loop. The closer is the cross with respect to the centre of the axes, the better is the driver feeling.

- low and constant steering input frequency: $f = 0.3\ Hz$

The steering wheel angle δ_{sw} and velocity u time histories from *MSC Adams*™simulations are provided as inputs to the single-track model, in order to compare the analysis results between the simple model and the full vehicle model.

In Figure 7, the steering torque M_S^* is represented as function of the lateral acceleration a_y: the range is $a_y = \pm 0.5\ m/s^2$. In the ideal case, the values of M_S^* at null a_y should be symmetric with respect to the origin, meaning that the steering effort for turning left and right is equal and opposite. Actually, due to tyre characteristics, the upper and lower curves of the loop (representing respectively right and left turn) show an offset that matches with the value of $M_{S,st}^*$ (computed according to Equation 23), as reported in Table 3. This is experienced by the driver as a different value of feedback torque on the steering wheel for left and right turn when performing the *weave test*. This result is meaningful, since it gives evidence to the fact that tyre characteristics' offsets (due to ply-steer and conicity) do have an influence on vehicle's on-centre handling.

The steering wheel angle-lateral acceleration (δ_{sw}-a_y) plots (which are not reported)

Table 3. Values of steering torque M_S^* at null lateral acceleration for left and right turn, from *MSC Adams*™ weave test simulation. Comparison with $M_{S,st}^*$ offset.

Tyre set	φ_r $[rad]$	$M_{S,st}^*$ $[Nm]$	*MSC Adams*™ $M_S^*(0)$ right $[Nm]$	*MSC Adams*™ $M_S^*(0)$ left $[Nm]$
Normal	0.00	−0.605	10.2	−11.3
Mod-A	0.00	−5.135	5.8	−16.1
Mod-B	0.00	3.606	14.7	−7.5
Buffed	0.00	3.138	18.3	−12.0
Normal	0.02	−9.958	1.0	−20.6
Mod-A	0.02	−14.695	−3.56	−25.5
Mod-B	0.02	−6.069	5.2	−17.0
Buffed	0.02	−10.763	4.85	−25.5

show a steering wheel offset at null a_y which is smaller than 1 deg with all the tyre sets, hence it is difficult to be perceived by the driver. Therefore, during a *weave test*, the driver is more likely to report subjective impressions on the steering feedback (described with the objective metrics M_S^* represented in Figure 7), rather than on the steering wheel angle offset.

Let us consider Table 3. We can see that the best set of tyres are *Mod-B*, as rated by the subjective-objective evaluation addressed in the previous Section. Actually, they have the least value of $M_{S,st}^*$ on banked road ($\varphi_r = 0.02 rad$). The opposite occurs for *Mod-A* tyres. It seems that the derived formulae are able to describe the actual performance of tyres.

6. Running on rough road

The effects of road irregularity on straight-ahead running have been examined, by considering two-tracks ground excitation as done in [25], with the purpose of estimating the variance of wheels' normal load, straight-driving lateral-slip angles (α_1 and α_2) and lateral displacement of vehicle's body (y). The computed estimations have then been compared to the standard deviations obtained from *MSC Adams*™ full vehicle simulations. The same *straight line maintaining test* employed in section 4.1 has been simulated with different sets of tyres on three flat road types, characterised by different irregularities (according to ISO8608 classification of road unevenness power spectral densities [26,27]).

The analysis can be found in [28] and is not reported in this paper. Nevertheless, the outcome is that the steady-state solutions (computed with Equations 17-18) appear to be kept also when the road roughness is introduced, which results just in irregularity superimposed to the steady-state solutions. Moreover, the amplitude of vehicle's body lateral displacement y is prone to depending mostly on vehicle and suspension characteristics, rather than on the specific set of tyres.

7. Suspension parameters affecting straight-ahead running

The straight-driving offsets pertaining to steering wheel angle δ_{st}, vehicle side-slip angle β_{st} and steering torque $M_{S,st}^*$ - defined respectively in Equations 19, 21 and 23 - can be rewritten in a more compact fashion in order to shed light on the influence of wheel alignment and specific tyre characteristics on vehicle pull.

In order to do so, the dependence of effective axle cornering stiffness on static toe Ψ_{i0} and camber γ_{i0} can be emphasised by gathering together the different contributions of Equation 3:

$$\begin{aligned} C_{el,AL,i} =& 1 + C_{roll,i} - C_{susp,i} + C_{steer,i} + \\ &+ \sigma_i \frac{l}{l - a_i} \cdot \left[\xi_{\alpha,i} \left(-\alpha_{ply,iL} + \alpha_{ply,iR} \right) + \xi_{\gamma,i} \left(-\gamma_{con,iL} + \gamma_{con,iR} \right) \right] \end{aligned} \tag{26a}$$

$$C_{el,\Psi,i} = \sigma_i \frac{l}{l - a_i} \cdot 2 \cdot \xi_{\alpha,i} \tag{26b}$$

$$C_{el,\gamma,i} = \sigma_i \frac{l}{l - a_i} \cdot 2 \cdot \xi_{\gamma,i} \tag{26c}$$

$$\Rightarrow \frac{1}{C^*_{eff,i}} = \frac{C_{el,AL,i}}{2C_{F\alpha,i0}} + \frac{C_{el,\Psi,i}}{2C_{F\alpha,i0}} \cdot \Psi_{i0} + \frac{C_{el,\gamma,i}}{2C_{F\alpha,i0}} \cdot \gamma_{i0}$$

In order to rewrite in a more compact form the aforementioned expressions for δ_{st}, β_{st} and $M^*_{S,st}$, the coefficients multiplying toe Ψ_{i0} and camber γ_{i0} are called respectively A_i, A_{1M} and B_i:

$$\begin{aligned} A_1 &= \left(\frac{C_{F\alpha,10R} - C_{F\alpha,10L}}{C_{F\alpha,10R} + C_{F\alpha,10L}} \right) + \frac{F_{z1}}{2C_{F\alpha,10}} \cdot C_{el,\Psi,1} \cdot \varphi_r \\ A_{1M} &= -\left(\frac{C_{M\alpha,1R} - C_{M\alpha,1L}}{C_{M\alpha,1R} + C_{M\alpha,1L}} \right) + \frac{F_{z1} \cdot n}{C_{M\alpha,1R} + C_{M\alpha,1L}} \cdot C_{el,\Psi,1} \cdot \varphi_r \\ B_1 &= \left(\frac{C_{F\gamma,10R} - C_{F\gamma,10L}}{C_{F\alpha,10R} + C_{F\alpha,10L}} \right) + \frac{F_{z1}}{2C_{F\alpha,10}} \cdot C_{el,\gamma,1} \cdot \varphi_r \\ A_2 &= \left(\frac{C_{F\alpha,20R} - C_{F\alpha,20L}}{C_{F\alpha,20R} + C_{F\alpha,20L}} \right) + \frac{F_{z2}}{2C_{F\alpha,20}} \cdot C_{el,\Psi,2} \cdot \varphi_r \\ B_2 &= \left(\frac{C_{F\gamma,20R} - C_{F\gamma,20L}}{C_{F\alpha,20R} + C_{F\alpha,20L}} \right) + \frac{F_{z2}}{2C_{F\alpha,20}} \cdot C_{el,\gamma,2} \cdot \varphi_r \end{aligned} \tag{27}$$

Furthermore, the coefficients expressing the contributions of side force and aligning moment offsets are condensed respectively into the terms C_i and C_{1M}:

$$\begin{aligned} C_1 &= \left(\frac{F_{y0,1R} + F_{y0,1L}}{C_{F\alpha,10R} + C_{F\alpha,10L}} \right) \\ C_{1M} &= \left(\frac{M_{z0,1R} + M_{z0,1L}}{C_{M\alpha,1R} + C_{M\alpha,1L}} \right) \\ C_2 &= \left(\frac{F_{y0,2R} + F_{y0,2L}}{C_{F\alpha,20R} + C_{F\alpha,20L}} \right) \end{aligned} \tag{28}$$

Finally, the coefficients concerning road cross slope φ_r are called:

$$\begin{aligned} D_1 &= \frac{F_{z1}}{C^*_{eff,1,AL}} \\ D_2 &= \frac{F_{z2}}{C^*_{eff,2,AL}} \\ E_{1M} &= C_{el,AL,1} \cdot F_{z1} \cdot \varphi_r \cdot \left(\frac{n}{C_{M\alpha,1R} + C_{M\alpha,1L}} + \frac{1}{2C_{F\alpha,10}} \right) \end{aligned} \tag{29}$$

Hence, we can write

- Steering angle: from Equation 19, with the approximations of Equations 17-18:

$$\delta_{st} = \left[-\Psi_{10} \cdot A_1 - \gamma_{10} \cdot B_1 - C_1 + \Psi_{20} \cdot A_2 + \gamma_{20} \cdot B_2 + C_2 \right] + \left(-D_1 + D_2 \right) \varphi_r \tag{30}$$

- Vehicle side-slip angle : from Equation 21, with the approximations of Equation 18:

$$\beta_{st} = \Psi_{20} \cdot A_2 + \gamma_{20} \cdot B_2 + C_2 + D_2 \varphi_r \tag{31}$$

- Steering torque: since static toe Ψ_{i0} and static camber γ_{i0} have a non-negligible influence on the effective axle aligning moment characteristic, this latter is introduced by analogy with the effective axle side force defined in Equations 2-7, neglecting the effect of camber (the difference between left and right camber characteristics is small). Under the assumption that the pneumatic trail relationship holds constant also for the effective axle characteristics, namely:

$$-\frac{C_{M\alpha,eff,i}}{C^*_{eff,i}} := t_0 = -\frac{C_{M\alpha}}{C_{F\alpha}} \tag{32}$$

the effective axle aligning moment reads:

$$M_{z,i} = -C_{M\alpha,eff,i} \cdot \alpha_i + M_{z0,i} \tag{33}$$

with:

$$\begin{aligned} C_{M\alpha,eff,i} &= \frac{C_{M\alpha,iL} + C_{M\alpha,iR}}{1 + C_{roll,i} - C_{susp,i} + C_{steer,i} + C^*_{\Delta F_z,i}} \\ M_{z0,i} &= C_{M\alpha,eff,i} \cdot \left[\left(\frac{M_{z0,iR} + M_{z0,iL}}{C_{M\alpha,iR} + C_{M\alpha,iL}} \right) - \Psi_{i0} \cdot \left(\frac{C_{M\alpha,iR} - C_{M\alpha,iL}}{C_{M\alpha,iR} + C_{M\alpha,iL}} \right) \right] \end{aligned}$$

Therefore, the straight-driving steering torque offset can be written from Equation 23 (introducing the approximations of Equations 17-18) as:

$$M^*_{S,st} = -C_{M\alpha,eff,1} \cdot \left[\Psi_{10} \cdot (A_1 + A_{1M}) + C_1 + C_{1M} + E_{1M} \right] \tag{34}$$

The front single tyre's Ply-steer Residual Aligning Torque $PRAT_1$, that is usually considered a cause of vehicle pull [1], is related to the factors C_1 and C_{1M}

appearing in Equation 34:

$$
\begin{aligned}
& C_{M\alpha,1} \cdot (C_1 + C_{1M}) = \\
& = \frac{C_{M\alpha,1}}{2C_{F\alpha,10}} (F_{y0,1R} + F_{y0,1L}) + M_{z0,1R} + M_{z0,1L} \\
& \rightsquigarrow 2 \cdot PRAT_1
\end{aligned}
$$

8. Applicability of the derived analytical formulae and early experimental substantiation

We have seen that, by the validated analytical formulae presented above, the steering angle δ_{st}, the vehicle side-slip angle β and the steering torque M_S^* can be computed analytically with reasonable accuracy.

The problem is now to use said formulae to set properly tyre and vehicle parameters.

Solving this problem requires a dedicated research that will follow the one presented in this paper. We provide here some basic hints that could be used as starting statements for an envisaged future scientific project.

In vehicle dynamics, as in other engineering fields, the theoretical contributions have to be substantiated by proper experimental activity. We attempt here an early experimental substantiation, based on the experience gained in a preliminary subjective-objective investigation, already addressed in Section 4.3.

8.1. Applicability

During straight-ahead motion we would like to have

- $\beta_{st} = 0$: null vehicle side-slip angle (no *dog-tracking* straight motion)
- $M^*_{S,st} = 0$: no steering torque is generated by tyres, so the driver does not have to apply any torque (or *pull*) on the steering wheel to maintain the straight motion
- $\delta_{st} = 0$: the steering wheel does not have angular displacement (or *misalignment*)

Common experience [1] seems addressing that all the above conditions are hard, or impossible, to be achieved. Let us check whether this fact is reproduced by our analytical formulae. The equations to be considered are Equations 30-31, 34 whose coefficients are reported in Equations 27-29. The values of such coefficients are reported in Table 4. The Table shows that the coefficients multiplying static camber γ_{i0} (namely B_1 for front and B_2 for rear) are significantly smaller than the coefficients multiplying static toe Ψ_{i0} (namely A_1, A_{1M} and A_2). In addition, they are null in case the road cross slope φ_r is null. Therefore, the influence of static camber γ_{i0} on straight-driving offsets can be neglected. Only the influence of front and rear static toe is considered henceforth.

The problem statement, integrated by the above analysis, is thus

$$
\begin{cases}
\beta_{st} = \Psi_{20} \cdot A_2 + C_2 + D_2 \varphi_r = 0 \\
\delta_{st} = [-\Psi_{10} \cdot A_1 - C_1 + \Psi_{20} \cdot A_2 + C_2] + (-D_1 + D_2)\, \varphi_r = 0 \\
M^*_{S,st} = -C_{M\alpha,eff,1} \cdot \left[\Psi_{10} \cdot (A_1 + A_{1M}) + C_1 + C_{1M} + E_{1M} \right] = 0
\end{cases}
$$

Table 4. Values of straight-driving offsets coefficients. Road cross slope $\varphi_r = 0.02\ rad$.

Tyre ID	A_1	A_{1M}	B_1	C_1	C_{1M}	E_{1M}	A_2	B_2	C_2
Normal	14.20e-3	-7.80e-3	1.16e-3	1.48e-3	-1.38e-3	1.74e-3	22.22e-3	1.54e-3	1.16e-3
Mod-A	23.81e-3	-18.31e-3	1.15e-3	1.50e-3	-0.59e-3	1.69e-3	35.59e-3	1.53e-3	1.12e-3
Mod-B	9.34e-3	-1.44e-3	1.11e-3	1.25e-3	-1.87e-3	1.63e-3	33.20e-3	1.48e-3	1.09e-3
Buffed	-2.58e-3	-1.66e-3	0.88e-3	1.52e-3	-1.77e-3	1.06e-3	10.00e-3	0.91e-3	1.29e-3

Now let us imagine that we need to compute the front and rear toe angles (Ψ_{10}, Ψ_{20}), given the elastokinematics and tyre characteristics of the vehicle. We immediately see that there are three equations with two unknowns, namely Ψ_{10} and Ψ_{20}.
Thus the problem cannot be solved, as common experience states.

We could still try to set *both tyres characteristics and toe angles*. This, in principle, could be done mathematically but, in the cases examined in Table 4, computed values of Ψ_{10} and Ψ_{20} are too big to be practically adopted. So also this approach seems unsuccessful, as common experience suggests.

Despite the two unsuccessful derivations, we can find a proper way to apply the derived analytical formulae. Since β_{st} and δ_{st} are very small, we could focus our attention on the steering torque $M^*_{S,st}$, the only variable that is clearly perceived by the driver.
Setting $\Psi_{10} = 0$, the third Equation in the above system of equations becomes

$$C_1 + C_{1M} + E_{1M} = 0 \tag{35}$$

Now *it is possible to find a tyre parameter setting that sets to zero the steering torque* $M^*_{S,st}$.
As an example, the *Mod-B* tyre of Table 4 is considered. The tyre characteristics at the front are slightly adjusted:

$C_{F\alpha,10}\ [N/rad]$	$\uparrow 1\%$
$F_{y0,1}\ [N]$	$\downarrow 20\%$
$C_{M\alpha,1}\ [Nm/rad]$	$\downarrow 13\%$
$M_{z0,1}\ [Nm]$	$\uparrow 23\%$

By such modified tyre characteristics, the steering torque $M^*_{S,st}$ is set to zero.

Summarising, for applicability, all of the formulae derived in the paper could be shrunk into Equation 35 that allows the setting of vehicle and tyre parameters at the front axle.

8.2. Early substantiation

We have mentioned that Equation 35 is the most important of the paper as far as the applicability is concerned. The values of the terms of Equation 35, namely C_1, C_{1M} and E_{1M}, are given in Table 4. The Table refers to the four tyres that were taken into consideration for the subjective-objective validation, addressed in Section 4.3. From Table 4 we see that none of the tyres satisfies Equation 35. The residuals of

Equation 35 are respectively $1.84e-3$, $2.60e-3$, and $1.01e-3$ for *Normal*, *Mod-A* and *Mod-B* tyres. The smallest residual belongs to *Mod-B* tyre and the biggest residual to *Mod-A* tyre. The bigger the residual the further the satisfaction of Equation 35. Again, as highlighted in the validation Section 4.3, the *Mod-B* tyre performed as the best one, the *Mod-A* tyre as the worst one.

9. Conclusions

The paper has presented a relatively simple but unreferenced road vehicle model for deriving the relevant parameters pertaining to straight-ahead motion. The Handling Diagram theory has been revised and updated, taking into account the full tyre characteristics and road cross slope.

The derived analytical linear model provides the following steady-state variables

- steering wheel angle
- lateral slips at front and rear axles
- steering wheel torque

The influence of wheel static camber and toe on the above stated variables is highlighted. The analytical formulae are validated by means of a full *MSC Adams*$^{\text{TM}}$ vehicle model, with satisfactory results. Validations refer not only to steady-state motion but also to both weave motion and lateral drift at null-steering. Additionally, a preliminary subjective-objective experimental validation seems confirming the ability of the derived analytical formulae to describe tyre performance.
The relationship between on-centre handling and tyre parameters has been highlighted by means of analytical exact formulae.
By means of the derived analytical formulae, given the vehicle, the technical specifications for tyres can be derived. Alternatively, given the tyre, the static wheel angles could be tuned, provided that they exist.
A proper tyre design may allow to make null the steering torque during straight-ahead driving.

The derived analytical formulae seem very effective to gain a sound insight into the straight-ahead running behaviour of road vehicles.

References

[1] Pottinger MG. Pull: The science of a nuisance. Tire Science and Technology. 2013 Jan-Mar;41(1):40–59.
[2] Lindenmuth B E. Tire conicity and ply steer effects on vehicle performance. SAE Technical Paper 740074. 1974;.
[3] Cho Y G. Steering pull and drift considering road wheel alignment tolerance during high speed driving. International Journal of Vehicle Design. 2010;54(1):73–91.
[4] Topping R W. Tire induced steering pull. SAE Technical Paper 750406. 1975;.
[5] Pottinger MG. Tire/vehicle pull: An introduction emphasizing plysteer effects. Tire Science and Technology. 1990 Jul-Sep;18(3):170–190.
[6] Lee J H. Analysis of tire effect on the simulation of vehicle straight line motion. Vehicle System Dynamics. 2000;33(6):373–390.
[7] Matyja FE. Steering pull and residual aligning torque. Tire Science and Technology. 1987 Jul-Sep;15(3):207–240.
[8] Mundl R, Fischer M, Wajroch M, Lee S W. Simulation and validation of the ply steer

residual aligning torque induced by the tyre tread pattern. Vehicle System Dynamics. 2005;43(Supplement):434–443.
[9] Ohishi K, Suita H, Ishihara K. The finite element approach to predict the plysteer residual cornering force of tires. Tire Science and Technology. 2002 Apr-Jun;30(2):122–133.
[10] Murakoshi H, Ide H, Nishihata S. An approach to vehicle pull using a tire finite element model. Tire Science and Technology. 1992 Oct-Dec;20(4):212–229.
[11] Murari T B, Lima D M, Zebende G F, Moret M A. Vehicle steering pull: from product development to manufacturing. Product: Management & Development. 2016 Jun; 14(1):22–31.
[12] Yamazaki S, Fujikawa T, Suzuki T, Yamaguchi I. Influence of wheel alignment and tire characteristics on vehicle drift. Tire Science and Technology. 1998 Jul-Sep;26(3):186–205.
[13] Yu H J. Tire/suspension aligning moment and vehicle pull. Tire Science and Technology. 2000 Jul-Sep;28(3):157–177.
[14] Pacejka HB. Tire and vehicle dynamics. 3rd ed. Amsterdam (NL): Elsevier; 2012.
[15] Mastinu G. Road and off-road vehicle system dynamics. Boca Raton (FL): CRC Press - Taylor & Francis Group; 2014. Chapter 11, Conceptual Design of Road Vehicles Related to Dynamics; p. 329–394.
[16] Schiehlen W. Road and off-road vehicle system dynamics. Boca Raton (FL): CRC Press - Taylor & Francis Group; 2014. Chapter 2, Vehicle Models and Equations of Motion; p. 13–44.
[17] Gim G. Road and off-road vehicle system dynamics. Boca Raton (FL): CRC Press - Taylor & Francis Group; 2014. Chapter 37, Subjective and Objective Evaluations of Car Handling and Ride; p. 1395–1476.
[18] Pfeffer P, Harrer M. On-centre steering wheel torque characteristics during steady state cornering. SAE Technical Paper. 2008 Apr;.
[19] Mitschke M. Dynamik der Kraftfahrzeuge - Band C: Fahrverhalten. Berlin (DE): Springer-Verlag; 1990.
[20] Harrer M, Pfeffer P. Steering handbook. Cham (CH): Springer; 2017.
[21] Matschinsky W. Road and off-road vehicle system dynamics. Boca Raton (FL): CRC Press - Taylor & Francis Group; 2014. Chapter 21, Suspension Systems; p. 727–768.
[22] Kageyama I. Road and off-road vehicle system dynamics. Boca Raton (FL): CRC Press - Taylor & Francis Group; 2014. Chapter 25, Steering System; p. 919–942.
[23] Salaani MK, Heydinger GJ, Grygier PA. Experimental steering feel performance measures. SAE Technical Paper. 2004;(2004-01-1074).
[24] International Organization for Standardization. Road vehicles: Test method for the quantification of on-centre handling - part 1: Weave test. SS-ISO13674-1; 2010.
[25] Mitschke M. Dynamik der kraftfahrzeuge - Band B: Schwingungen. Berlin (DE): Springer-Verlag; 1990.
[26] International Organization for Standardization. Mechanical vibration: Road surface profiles - Reporting of measured data. ISO8608; 2016.
[27] Hrovat D. Road and off-road vehicle system dynamics. Boca Raton (FL): CRC Press - Taylor & Francis Group; 2014. Chapter 31, Active and Semi-Active Suspension Control; p. 1179–1226.
[28] Lattuada A. Straight ahead running of road vehicles [master's thesis]. Politecnico di Milano; 2018.
[29] MSC Software. Adams/Tire; 2015. Available from: https://simcompanion.mscsoftware.com/infocenter/.

Appendix A. Effective axle side force derivation

A.1. Approximation of tyre side force

A comparison is made between a linearisation of tyre side force $F_y = F_y(\alpha, \gamma, F_z)$ and the approximation adopted by Pacejka [14].

- **Linearisation**:

$$\begin{aligned} F_y = &\left(F_y \Big|_{\substack{\alpha=0 \\ \gamma=0 \\ F_z=F_{z0}}} \right) + \left(\frac{\partial F_y}{\partial \alpha} \Big|_{\substack{\alpha=0 \\ \gamma=0 \\ F_z=F_{z0}}} \right) \cdot \alpha + \left(\frac{\partial F_y}{\partial \gamma} \Big|_{\substack{\alpha=0 \\ \gamma=0 \\ F_z=F_{z0}}} \right) \cdot \gamma + \\ &+ \left(\frac{\partial F_y}{\partial F_z} \Big|_{\substack{\alpha=0 \\ \gamma=0 \\ F_z=F_{z0}}} \right) \cdot (F_z - F_{z0}) = F_{y0} + C_\alpha \cdot \alpha + C_\gamma \cdot \gamma + C_{F_z} \cdot \Delta F_z \end{aligned} \tag{A1}$$

- **Approximation from Pacejka [14]**:

$$F_y = F_{y0} + (C_\alpha + \xi_\alpha \cdot \Delta F_z) \cdot \alpha + (C_\gamma + \xi_\gamma \cdot \Delta F_z) \cdot \gamma \tag{A2}$$

Comparing the approximations with a Magic Formula characteristic curve (for different lateral-slip angles $\alpha \in [-1\,\text{deg}, 1\,\text{deg}]$, three camber angles $\gamma = [-1\,\text{deg}, 0\,\text{deg}, 1\,\text{deg}]$ and three loads $F_z = [0.95, 1, 1.05] \cdot F_{z0}$), the approximation of Pacejka results in a smaller error with respect to the linearisation, as it can be observed in Figure A1. The error is defined using the difference with respect to the Magic Formula curve:

$$err_{abs} = \frac{F_{y,MF} - F_{y,approx}}{F_{y,MF}}$$

A.2. Effective axle side force

It is assumed that the linearisation coefficients $\xi_{\alpha,i}$ and $\xi_{\gamma,i}$ are equal for left and right wheels:

$$\begin{aligned} \xi_{\alpha,iL} &= \xi_{\alpha,iR} = \xi_{\alpha,i} \\ \xi_{\gamma,iL} &= \xi_{\gamma,iR} = \xi_{\gamma,i} \end{aligned}$$

On the other hand, the cornering stiffness and camber coefficient are considered to be different for left and right tyres, in order to accommodate the description of asymmetric properties:

$$\begin{aligned} C_{F\alpha,iL/R} &= C_{F\alpha,i0L/R} \pm \xi_{\alpha,i} \cdot \Delta F_{z,i} \\ C_{F\gamma,iL/R} &= C_{F\gamma,i0L/R} \pm \xi_{\gamma,i} \cdot \Delta F_{z,i} \end{aligned} \tag{A3}$$

Therefore - introducing the ply-steer and conicity equivalent angles, the cornering stiffness and camber coefficient and the static toe and camber - the side forces for axle

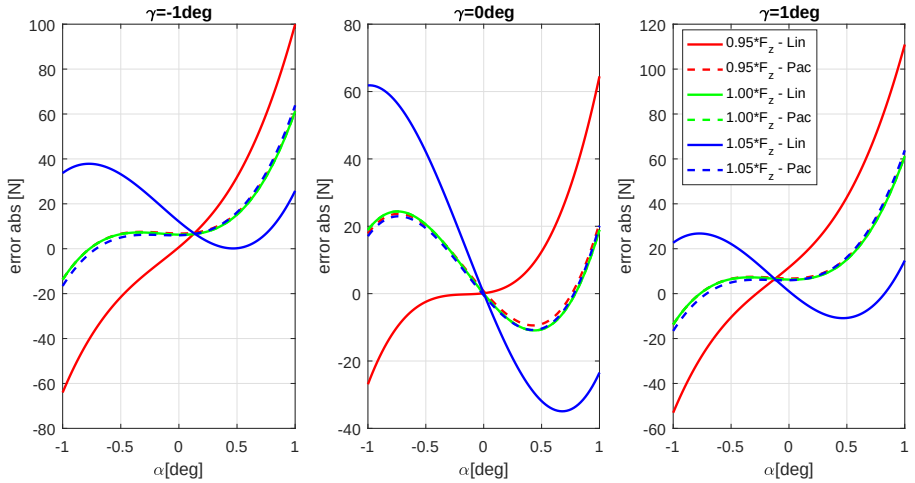

Figure A1. Error of the linearisation (*Lin*, solid lines) and Pacejka's approximation (*Pac*, dashed lines) of F_y with respect to Magic Formula curves, for different normal loads, camber angles and lateral-slip angles. The dashed lines are almost overlapping, which means that the Pacejka's approximation is better than the canonical linearisation.

i (for left L and right R side) can be written as:

$$\begin{aligned} F_{y,iL} = \quad & (C_{F\alpha,i0L} + \xi_{\alpha,i}\Delta F_{z,i})(\alpha_i - \Psi_{i0} + \alpha_{ply,iL}) + \\ & + (C_{F\gamma,i0L} + \xi_{\gamma,i}\Delta F_{z,i})(\gamma_{r,i} - \gamma_{i0} + \gamma_{con,iL}) \\ F_{y,iR} = \quad & (C_{F\alpha,i0R} - \xi_{\alpha,i}\Delta F_{z,i})(\alpha_i + \Psi_{i0} + \alpha_{ply,iR}) + \\ & + (C_{F\gamma,i0R} - \xi_{\gamma,i}\Delta F_{z,i})(\gamma_{r,i} + \gamma_{i0} + \gamma_{con,iR}) \end{aligned} \tag{A4}$$

It is possible to introduce the average of left and right cornering stiffness and camber coefficient $C_{F\alpha,i0}$ and $C_{F\gamma,i0}$.

The side force $F_{y,i}$ for the axle i is given by the sum of left and right forces.

The following terms are now to be substituted in the previous equation:

$$\gamma_i = \gamma_{r,i} = \tau_i \cdot \varphi \tag{A5}$$

$$\alpha_i = \alpha_{ai} + \Psi_{r,i} + \Psi_{sf,i} + \Psi_{c,i} \tag{A6}$$

where α_{ai} is the *virtual lateral-slip angle* [14], which is called α_i in the paper for conciseness.

$$\Psi_{r,i} = \varepsilon_i \cdot \varphi \tag{A7}$$

$$\Psi_{sf,i} = c_{sf,i} \cdot F_{y,i} \tag{A8}$$

$$\Psi_{c,i} = -\frac{F_{y,i}(n_i - t_{0,i})}{c_{\Psi,i}} \tag{A9}$$

where the terms of roll and load transfer follow from the steady-state cornering assumption, and are defined as function of the lateral force (or lateral acceleration):

$$\varphi = \frac{-h'}{k_{\varphi 1} + k_{\varphi 2} - mgh'} \cdot \frac{l}{l - a_i} F_{y,i} \tag{A10}$$

$$\begin{aligned}\Delta F_{zi} &= F_{y,i}\frac{l}{l-a_i}\sigma_i \\ \sigma_i &= \frac{1}{2s_i}\left(\frac{k_{\varphi i}}{k_{\varphi 1}+k_{\varphi 2}-mgh'}h' + \frac{l-a_i}{l}h_i\right)\end{aligned} \tag{A11}$$

By substituting all the previously listed terms into the axle's side force equation, it is possible to write:

$$\begin{aligned}F_{y,i} = {} & 2C_{F\alpha,i0}\cdot\alpha_{ai} + F_{y,i}\cdot(2C_{F\alpha,i0})\cdot\left[\varepsilon_i\cdot\frac{-h'}{k_{\varphi 1}+k_{\varphi 2}-mgh'}\cdot\frac{l}{l-a_i} + c_{sf,i} - \frac{(n_i-t_{0,i})}{c_{\Psi,i}}\right] + \\ & + F_{y,i}\cdot(2C_{F\gamma,i0})\cdot\left[\tau_i\cdot\frac{-h'}{k_{\varphi 1}+k_{\varphi 2}-mgh'}\cdot\frac{l}{l-a_i}\right] + \\ & + F_{y,i}\cdot\sigma_i\cdot\frac{l}{l-a_i}\cdot[\xi_{\alpha,i}\cdot(-2\Psi_{i0}+\alpha_{ply,iL}-\alpha_{ply,iR}) + \xi_{\gamma,i}\cdot(-2\gamma_{i0}+\gamma_{con,iL}-\gamma_{con,iR})] + \\ & + [C_{F\alpha,i0L}\cdot(\alpha_{ply,iL}-\Psi_{i0}) + C_{F\alpha,i0R}\cdot(\alpha_{ply,iR}+\Psi_{i0})] + \\ & + [C_{F\gamma,i0L}\cdot(\gamma_{con,iL}-\gamma_{i0}) + C_{F\gamma,i0R}\cdot(\gamma_{con,iR}+\gamma_{i0})]\end{aligned}$$

By grouping all the terms multiplying lateral force $F_{y,i}$ and dividing by $2C_{F\alpha,i0}$, the effective axle cornering stiffness (defined as the slope $C^*_{eff,i} = dF_{y,i}/d\alpha_{ai}$ and expressed by Equation 3) can be found as the reciprocal of the coefficient multiplying $F_{y,i}$ in the previous equation.

Appendix B. Tyre data

The data, provided by *Pirelli Tyre S.p.A.*, are referred to factory-new winter tyre sets. Measurements have been obtained by *Smithers RAPRA Inc.*, that performed tyre tests with an *MTS Flat-Trac*® system.

The data are represented graphically in Figure B1, normalised with respect to *Normal* set's characteristics for confidentiality reasons. They pertain to four different types of tyres:

- Normal: tyre without any modification
- Mod-A: tyre with modified tread in order to obtain positive PRAT
- Mod-B: tyre with modified tread in order to obtain negative PRAT
- Buffed: tyre with completely removed tread part

The different types of tyres were tested under four different loading conditions:

- $F_z = 4500N$: front axle tyre, nominal load
- $F_z = 2800N$: rear axle tyre, nominal load
- $F_z = 6400N$: front axle tyre, with load transfer during a braking event
- $F_z = 900N$: rear axle tyre, with load transfer during a braking event

The characteristics are approximated, in the neighbourhood of the front and rear nominal loads, with a piecewise interpolation of the data, with second order polynomials passing through three points:

- front axle tyre (in the neighbourhood of nominal load $F_z = 4500N$):
  polynomial passing through
  - data at $F_z = 2800N$

  - data at $F_z = 4500N$
  - data at $F_z = 6400N$
- rear axle tyre (in the neighbourhood of nominal load $F_z = 2800N$): polynomial passing through
  - data at $F_z = 900N$
  - data at $F_z = 2800N$
  - data at $F_z = 4500N$

The second order approximation formulae for the different tyre characteristics are reported in Equations B1-B4. They are intended to be used to compute the coefficients' values for small load variations around the data points. Therefore, the best fit of the available data is pursued rather than a realistic description of the behaviour. The second order polynomial is selected, since it ensures the passage through the three data points for the piecewise interpolation, without increasing unnecessarily the complexity of the problem.

$$C_{F\alpha,i0L/R} = p_{Cf,i0} + p_{Cf,i1} \cdot (F_{z,iL/R}) + p_{Cf,i2} \cdot (F_{z,iL/R})^2 \tag{B1}$$
$$C_{M\alpha,i0L/R} = p_{Cm,i0} + p_{Cm,i1} \cdot (F_{z,iL/R}) + p_{Cm,i2} \cdot (F_{z,iL/R})^2 \tag{B2}$$
$$F_{y0,iL/R} = p_{Fy,i0} + p_{Fy,i1} \cdot (F_{z,iL/R}) + p_{Fy,i2} \cdot (F_{z,iL/R})^2 \tag{B3}$$
$$M_{z0,iL/R} = p_{Mz,i0} + p_{Mz,i1} \cdot (F_{z,iL/R}) + p_{Mz,i2} \cdot (F_{z,iL/R})^2 \tag{B4}$$

The left and right tyres' offsets are computed from the data according to:

$$F_{y0,iR} = F_{ply,i} + F_{con,i} \tag{B5}$$
$$F_{y0,iL} = F_{ply,i} - F_{con,i} \tag{B6}$$
$$M_{z0,iR} = M_{ply,i} + M_{con,i} \tag{B7}$$
$$M_{z0,iL} = M_{ply,i} - M_{con,i} \tag{B8}$$

The tyre property files of the *MSC Adams*™full vehicle model have been created using the *PAC2002*[1] *Tire Data and Fitting Tool (TDFT)* of *MSC Adams/Tire* [29]. In this case, the tool has been used to compute realistic tyre parameters for steady-state pure lateral slip, i.e. lateral force F_y and aligning moment M_z with respect to lateral-slip angle α. The different tyres' linear data available, which have been introduced in this section, have been used as virtual test values, together with additional fictitious points outside the linear region from a default *PAC2002* tyre model provided in *MSC Adams*™. This operation has been performed in order to obtain tyre property files having both realistic coefficients and the desired linear characteristics and shifts, corresponding to the values of data in the pertaining range of lateral-slip angle.

Appendix C. Sign conventions

The sign convention chosen for this work is consistent with the *Pacejka's modified SAE* [14], represented in Figure C1. With this convention, when no offsets are considered,

[1] *PAC2002* is the latest version of a Magic Formula tyre model available in *MSC Adams/Tire*, developed according to [14].

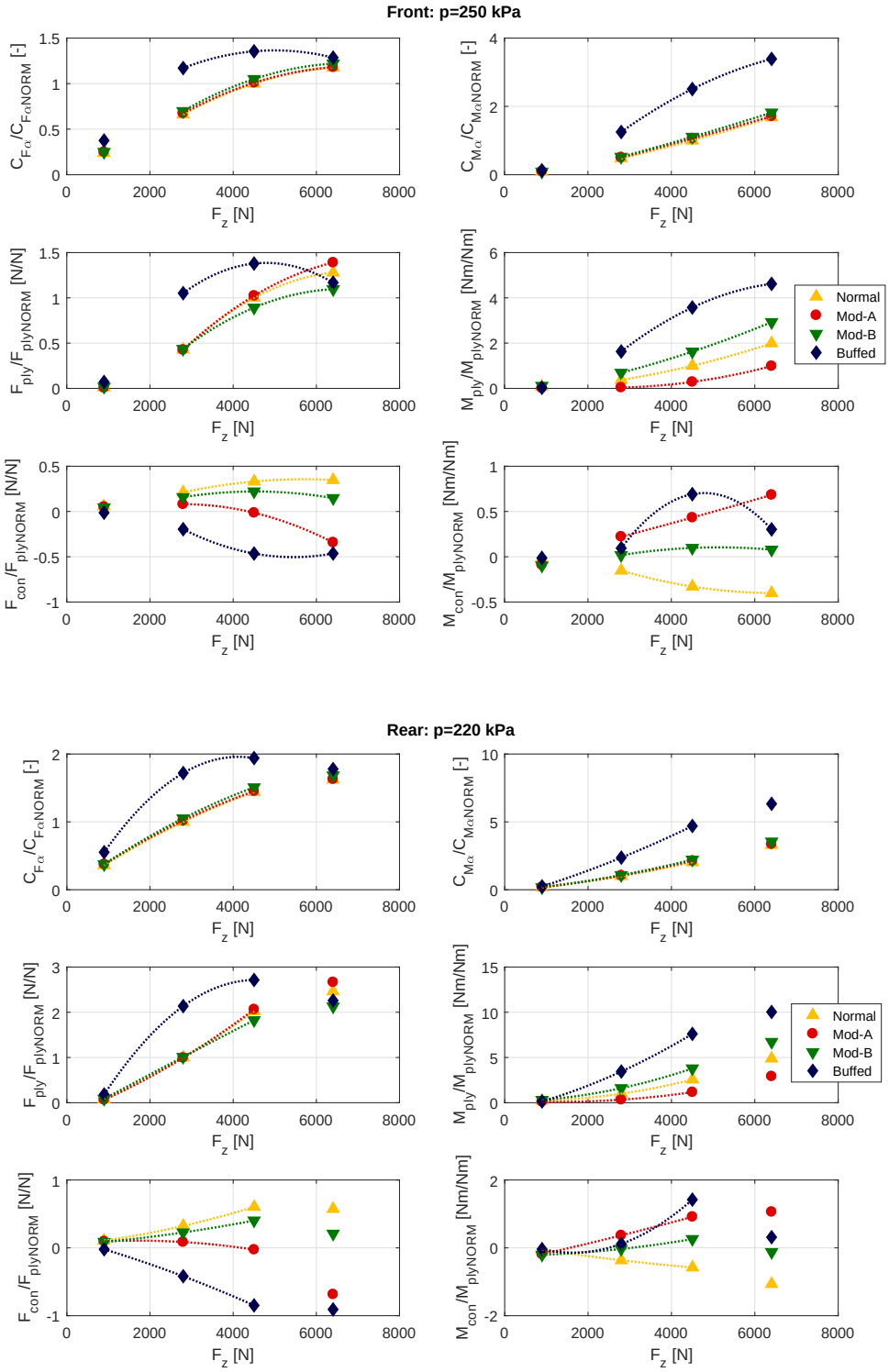

Figure B1. Tyre data, normalised with respect to *Normal* set characteristics. The polynomial interpolations (dotted lines) are used to compute tyre characteristics in the neighbourhood of nominal loads (front $F_z = 4500\ N$, rear $F_z = 2800\ N$).

side force is positive when lateral-slip angle is positive, while the opposite happens with aligning moment.

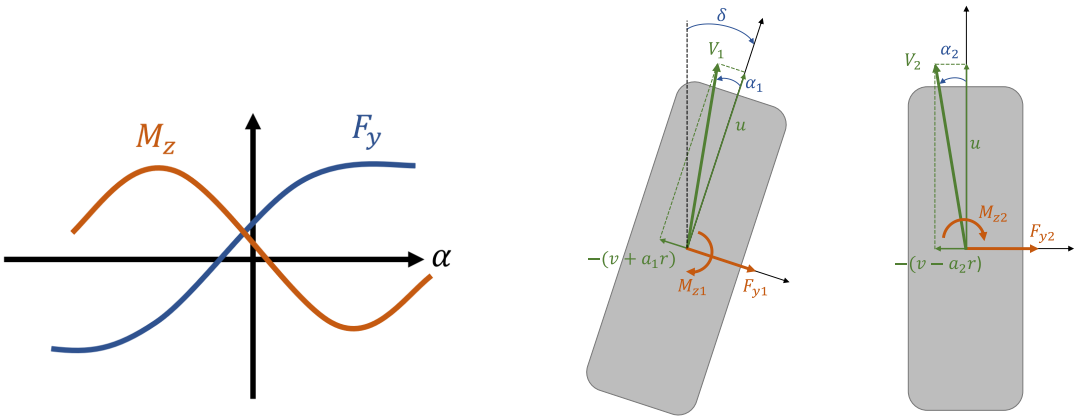

Figure C1. *Pacejka's modified SAE* sign convention for force, moment and wheel lateral-slip angle [14].

The sign convention for static toe and camber angles is reported in Figure C2.

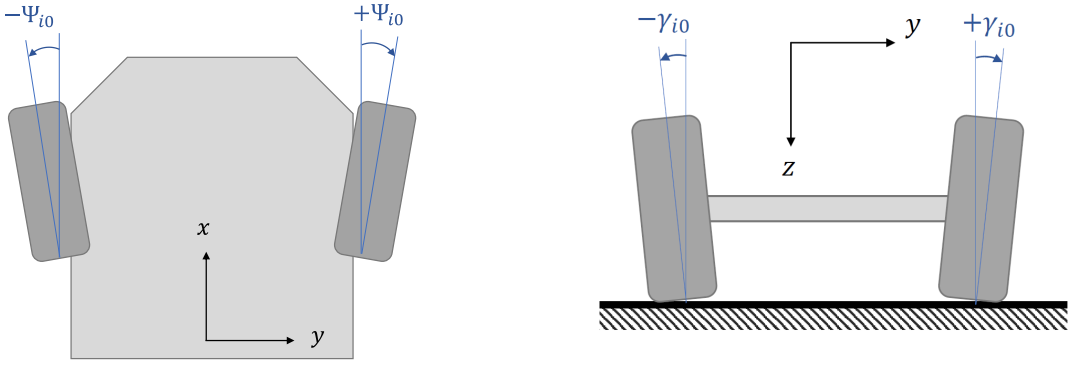

(a) Static toe.

(b) Static camber.

Figure C2. Sign convention for static toe and static camber angle.

Appendix D. Tyre and vehicle data

Tyre parameters and vehicle data are listed in Table D1.

Table D1. Tyre parameters and vehicle data.

Variable name	Description	Value	Unit
m_{tot}	Total mass	1488	kg
I_z	Yaw moment of inertia	2208.1	$kg\ m^2$
I_x	Roll moment of inertia	534.9	$kg\ m^2$
m_{t1}	Unsprung mass front (single wheel)	40	kg
m_{t2}	Unsprung mass rear (single wheel)	35	kg
l	Wheelbase	2.550	m
a_1	Distance CoG-Front axle	0.978	m
a_2	Distance CoG-Rear axle	1.572	m
h_G	CoG height	0.494	m
h_1	Front roll centre	0.0588	m
h_2	Rear roll centre	0.0796	m
h'	Distance roll axis-CoG	0.427	m
$2s$	Track width	1.460	m
k_1	Front suspension spring stiffness	20000	N/m
k_2	Rear suspension spring stiffness	24000	N/m
c_1	Front suspension damping (compression)	3800	Ns/m
c_2	Rear suspension damping (compression)	1300	Ns/m
$k_{\varphi 1}$	Front rolling stiffness	40544.2	Nm/rad
$k_{\varphi 2}$	Rear rolling stiffness	41851.7	Nm/rad
$c_{\varphi 1}$	Front roll damping	3508.9	$Nm\ s/rad$
$c_{\varphi 2}$	Rear roll damping	922.2	$Nm\ s/rad$
ε_1	Roll-steering coefficient (front)	-0.0245	
ε_2	Roll-steering coefficient (rear)	-0.0909	
τ_1	Roll-camber coefficient (front)	0.8912	
τ_2	Roll-camber coefficient (rear)	0.9137	
n	Caster offset	0.02	m
ξ_γ	Camber coefficient linearisation	1	$1/rad$
n_{st}	Steering ratio	13.03	
$C_{F\gamma}$	Side force camber coefficient	F_z	N/rad
$C_{M\gamma}$	Aligning moment camber coefficient	$0.1049 \cdot F_z$	N/rad

To the Reviewers of the Paper

Straight-ahead running of road vehicles - Analytical formulae including full tyre characteristics

Giampiero MASTINU, Alessandro LATTUADA, Giuseppe MATRASCIA

submitted to *Vehicle System Dynamics*

Milan, 30 September 2018

Dear Sirs

we are re-submitting our paper mentioned above for your consideration. We are grateful to the Reviewers for the time they have spent in providing us very useful hints to improve the quality of our paper.

We provide here some explanation on the changes that we made to answer the requests made by the reviewers.

Reviewer 1

The paper is well structured and is theoretically correct. It is as well a very complete study about “Nuisance”. However, the interest and applicability should be clarified.

“All of the cited papers do not resort to analytical modelling which, in our opinion, is crucial for establishing the actual influence of relevant parameters on performance. Our contribution can focus on an analytical model because the straight-ahead running can be dealt with by means of a relatively simple linear model”. This point should be clarified at the end of the paper; for instance, by means of a final list of variables related to steering wheel angle, steering wheel torque and lateral slips at front and rear axles. Identify the contribution with regard to previous studies.

We have added Section 8 at the end of the paper to discuss the Reviewer’s requests referring to applicability. We agree with the reviewer to clarify better how to exploit the mathematical analytical expressions.

Referring to the contribution of previous studies, we have added some text in the

mastinu@mecc.polimi.it
Politecnico di Milano, via Privata Giuseppe La Masa, 1, 20156 Milano MI
Ph. +39 02 2399 8289

Introduction. The new text is written in red color.

“A proper tyre design may allow to make null the steady-state steering wheel torque by setting properly the static toe angles”. Is this a real possibility from the point of view of tyre manufacturers? it would be very interesting if this sentence were clarified, mainly considering the affiliation of one of the authors to a tyre manufacturer, .

We have better clarified our statement with respect to the previous version of the paper. Actually, by means of the analytical equations that are given, a method can be developed to select tyre main parameters to make null the steering wheel torque. The discussion is introduced in the mentioned Section 8 at the end of the paper. The new text is written in red color.

Reviewer: 2

Comments to the Author

The papers present an application of a classical and well-known model to a specific problem (running) and its different causes, The attempt to obtain an analytical solution is commendable since it - at least - will provide an insight of the actual dynamic. I would suggest to compare the obtained results not only to Adams simulations but also with some experimental data or results from other simulations that can be found on the references.

We thank the reviewer for his/her valuable advice. Due to the length of the paper we decided to describe the experimental results in another article. The actual experimental tests are expensive and are being funded. Nonetheless we can already provide some experimental result. We already pointed out in the paper (and now highlighted better) that the subjective rating of the performance of the four tyres is fully consistent with computations. We have added

-a sub-section (4.3 Subjective experimental validation) and

-a sentence at the end of Section 5 for highlighting the subjective rating

-an early substantiation in Section 8.

Referring to other references, we added a sentence in the Introduction.

The new text is written in red color.

We do recommend a review in spelling and grammar. For instance, look at page 2 line 21 "desalt with" and maybe it would be "dealt with".

We have re-read the paper and removed some typos. We thank the reviewer for the advice.

Reviewer: 3

Comments to the Author

content

- page 1 line 29: considering suspension and steering, typically you will find dry friction at different places which can not be linearized in the strong sense of system dynamics. Please explain why these effects are neglected here anyway

We thank the reviewer because with his/her advice has allowed us to be more precise in stating our results.

We have slightly modified Section 3.3 in which we address the moment acting at the steering system produced by external tyre moments and forces. Thus we deal with a moment (that we have called ‘steering moment’) that is applied to the steering system from outside the vehicle. In other words, we refer to *external* forces generated by the tyres that cause the moment acting at the steering system and disregard the *internal* forces inside the steering system. This allows us to avoid mentioning and including refined models of the steering systems in which friction play a crucial role.

We argue that our simple model of the steering system may be used for a preliminary assessment. Resorting to the book by Pfeffer and Harrer (Steering Handbook), we see at pag. 109 that a complex steering system with friction behaves almost as a simple steering system without friction.

If the friction (stick-slip effect) would have been important, we would have missed the good correlation between subjective and objective results, referring to the four tyres that have been tested.

- page 3 equation (3): please explain why C_susp,i is

taken negative. Sign convention?

The minus sign was given in [13,14] and means that such a term can increase the effective axle cornering stiffness, contrary to other terms (C_{roll}, C_{steer}, $C_{\Delta Fz}$) that usually decrease it.

- page 7 equation (16): to me, it doesn't seem necessary (and possible) here to explain the fundamentals of the MBS code Adams by just one equation. Leave it away and refer to the literature

We have modified the equation according to the Reviewer's advice.

- page 8 line 56: 0.3g seems to me too large for the linear range (and is not needed either in the context of the paper). Many drivers rarely reach 0.3g

We agree with the reviewer that 0.3g is a limit value. Since the friction between tyre and ground is nearly 1 in our case, the tyre linear characteristics are linear up to 0.3 Fzmax. Thus, the value of the lateral slip corresponding to 0.3g is acceptable in the cases shown in the paper.

Obviously, should the friction be lower than 1, the limit value of 0.3g would be not acceptable. According to what is reported in the fundamental book by Mitschke, 0.3g is the very limit of the linear range of the handling diagram if friction is equal nearly to 1. (We agree with the Reviewer that such a lateral acceleration is usually exceeded by normal drivers only running on motorway on-ramps or off-ramps). We checked the handling diagram and, since the shape is linear, it means that the two effective axle characteristics are linear which implies that at least tyres can still be considered linear in the given range.

- page 9 equation (23): this relationship completely disregards friction, aligning by weight, steady-state nonlinearities, and eigendynamics in the steering system (mechanics + electric or hydraulic power assist). Please add some explanation why all this can be disregarded here

Please refer to our answer to the Reviewer's question referring to page 1 line 29. We disregard the steering system and focus our attention on the *external*

moment applied to it.

- page 10 chapter 4.1: please explain how 'straight line' is achieved in Adams. Closed loop (track distance control by driver model?) Open loop?

We thank the reviewer for his/her question that allowed us to better clarify what was explained at page 10 in lines 45-46. The simulation option in MSC Adams is called *Straight-Line event*/*Maintain*. Here it is possible to choose the *steering input* option *straight line*: in this way the software determines the steering input that maintains the vehicle along a straight path throughout the simulation. We have added a few sentences in order to further comment on our MSC Adams simulations.

- page 13, lines 16 to 21: longitudinal forces (esp. with front-wheel-driven vehicles) will slightly influence side forces and aligning torques ('combined slip'). Please explain why this can be neglected here

All of the simulations performed in the paper start with a given speed and then a coasting manoeuvre is attained. This corresponds to the tyre data that were measured at free rolling condition. The effect of rolling resistance is already taken into account in the tyre characteristics.

The PRAT, according to our experience, is measured today at free rolling condition only. The effect of longitudinal force could be dealt with in another paper, since the complexity of the model increases considerably. We did want to concentrate on an already complex phenomenon.

- page 13 line 33: camber influence on side force is not only given by camber-dependent share of weight force, but also by camber thrust. Please explain why this can be neglected here

We have included the camber thrust by referring to the static camber angle (γ_{io} in Eq. 5d).

- page 15 line 32: referring to the hysteresis in fig. 6, you seem to use a non-trivial steering system model in Adams which includes dry friction effects? In

order to compare to the simple Matlab model, I assume you pass over to this model the resulting steering (toe) angles of the wheels, rather than the steering wheel angle? If not, how do you get the hysteresis in the Matlab model? Please clarify.

We thank the Reviewer for his/her question that allows us to clarify better what we did. We used sometimes the word 'hysteresis' meaning actually loop or cycle.

Fig.6 is just the combination of two variables with phase lag. We have the sinusoidal input (M*s) and the resulting motion a_y. Due to the inherent dynamics of the vehicle, the acceleration a_y has a phase lag with respect to the input M*s.

No hysteresis (due e.g., to friction) is included into the Matlab model.

We have removed thus the improper 'hysteresis' term.

- page 22 Appendix A.1.: effectively, Pacejka's approximation is a partially *bilinear* expression, containing the products (∆Fz)*α and (∆Fz)*γ. It doesn't seem necessary to me to explain that this expression slightly differs from its strictly linearized version

We respectfully disagree with the Reviewer. There is a remarkable difference between the linearized expression of tyre characteristics and the Pacejka's approximation. With the Paceyka's approach the error does not depend on the vertical load, which is not the case for canonical linearization. This has a remarkable influence on model behaviour. Actually, wheel alignment angles are mainly in conjunction with the vertical loads. Making an error on them causes an error in the estimation of the influence of wheel alignments on model behaviour.

typos

- page 2 line 21: 'dealt'

thank you!

- page 21 line 55: Kraftfahrzeuge (capital K)

thank you, capital K is needed in German!

- page 25 line 5: four, not five different types of tyres

thank you!

terminology

- page 2 line 24: you mean 'tyre belt' instead of 'tyre tread'?

We did mean ‘tread’, because the ply-steer depends not only on tyre belt, but also on tyre tread pattern.

- page 6 line 19, page 8 line 28, etc.: to my knowledge, the term 'side-slip angle' refers to the full vehicle (and is what you call 'attitude' later on). With respect to the tire, it is simply 'slip angle'

Referring to the tyre, we have adopted ‘lateral-slip angle’. Actually, we may have at the tyre either longitudinal or lateral slips (and related angles). Referring to the vehicle, we have used “vehicle sideslip angle”, according to the terminology proposed by SAE J670_200801. We have modified the text in red color.

- page 10 line 41 etc: you are using terms 'ADAMS', 'MSC ADAMS', 'Adams' for the same software. Please use correct product name, optionally together with trade mark sign. Same holds for 'Matlab'

thank you! We have harmonized the softwares’ names both in text and figures.

- page 11 line 50 etc.: you are using 'δ_sw', 'δ_st', and 'δ_SW' for the steering wheel angle signal. Please harmonize

thank you! ('δ_sw' and 'δ_st' have different meanings)

formatting

- page 6 lines 54 to 56, page 8 lines 30 to 37 etc.: insert more distance between equations

thank you!

images

- page 4: please enlarge images. Annotation is barely readable

- page 4: the term 'single track' in the image (a) caption is misleading, since it clearly shows a two-track model with individual variables left/right

We thank the reviewer for his/her valuable effort in reviewing so closely the manuscript. We have changed the caption.

- page 23 fig. A1: two of the dashed lines cannot be seen

We have changed the caption and explained that the dashed lines are overlapping.

Best regards

Giampiero Mastinu
Alessandro Lattuada
Giuseppe Matrascia